INVESTIGATION OF RETINAL CHARACTERISTICS IN TREATED AMBLYOPIA

A thesis presented to the graduate faculty of
New England College of Optometry in partial fulfillment
of the requirements for the degree of Master of Science

Lindsey A. Wetherby

March, 2013

© Lindsey A. Wetherby
All rights reserved

The author hereby grants New England College of Optometry permission to reproduce and to distribute publicly paper and electronic copies of the thesis document in whole or in part.

INVESTIGATION OF RETINAL CHARACTERISTICS IN TREATED AMBLYOPIA

Lindsey A. Wetherby

This manuscript has been read and accepted by the
Thesis Committee in satisfaction of the
thesis requirement for the degree of Master of Science

3/29/2013
Date

Elise N. Harb, O.D., M.S.
Graduate Faculty Advisor

Stacey S. Choi, Ph.D.
Graduate Faculty Secondary Advisor

Robert Dunphy, O.D.
Thesis Committee Member

Erik M. Weissberg, O.D.
Thesis Committee Member

4-17-2013
Date

Nancy J. Coletta, O.D., Ph.D.
Director of Graduate Studies

New England College of Optometry

INVESTIGATION OF RETINAL CHARACTERISTICS IN TREATED AMBLYOPIA

Lindsey A. Wetherby

The New England College of Optometry, 2013

Abstract

Purpose: Though the deficit in amblyopia has traditionally been attributed to alterations in the primary visual cortex prior to the critical period of plasticity, recent advances in retinal imaging have allowed researchers to investigate any potential retinal alteration in amblyopia. Using optical coherence tomography (OCT), differences in retinal nerve fiber layer thickness (RNFLT) and macular thickness in amblyopic eyes have previously been investigated using optical coherence tomography (OCT), without much consensus. The aim of this study was to investigate RNFLT as well as the thickness of inner and outer retinal layers in the macula using OCT, in conjunction with the study of cone density and packing characteristics in the macula using adaptive optics (AO) fundus imaging.

Methods: 7 treated amblyopic subjects, with a range of residual amblyopia, and 4 age-matched (22-27y) emmetropic control subjects underwent binocular function assessment and imaging with a Fourier Domain OCT system (RTVue, RT-100). RNFLT was evaluated in four quadrants and globally surrounding the optic nerve. Thickness of the macula was evaluated in terms of outer retinal thickness (ORT) at four eccentricities (2- and 4-degree nasal and temporal eccentricities) from the fovea, and inner retinal thickness (IRT) at two eccentricities (4-degree nasal and temporal). Thickness data was analyzed for amblyopic and fellow eyes and from both eyes of the control subjects. Images of cone photoreceptors

obtained by AO imaging were analyzed for cone density and packing characteristics using Voronoi analysis.

Results: There were no significant differences in RNFLT between amblyopic and control eyes, nor between amblyopic and fellow eyes (p values>0.10) in any quadrant or globally (p values>0.10). IRT at the 4-degree temporal location was not significantly different between amblyopic and control eyes (p=0.24), nor between amblyopic and fellow eyes (p=0.73). However, the difference in IRT at the 4-degree nasal location approached significance (p=0.06), with amblyopic eyes being slightly thinner than control eyes (mean diff.=11.12 microns), but not between amblyopic and fellow eyes (p=0.12). Differences in ORT were significant between amblyopic and fellow eyes at the 2-degree nasal and temporal positions (p=0.03 and p=0.02, respectively), but not between amblyopic and control eyes at any location studied. Mean cone density was similar among all groups at all positions except at the 4-degree temporal location, where mean cone density was higher in amblyopic eyes as compared to controls. Voronoi analysis suggested that amblyopic eyes appear to have a more disorganized cone packing arrangement, especially at the 2- and 4- degree temporal positions.

Discussion: In this small preliminary study, while there were generally no significant differences in the inner retinal layers studied (IRT and RNFLT) in eyes with treated amblyopia compared to their fellow eyes or control eyes, there was a significant difference in ORT at 2-degree eccentricities from the fovea. It remains to be seen if these small but significant differences in retinal thickness are clinically significant. Unique to this study was the joint imaging of subjects with both OCT and AO systems. While some analyses suggested differences in cone density in amblyopic eyes in terms of increased density and increased disorganization of the photoreceptor array, these findings were slight and require increased subject number to verify. More investigation is warranted in both treated and un-treated amblyopes to detect if differences in the retina of eyes with a history of amblyopia exist and whether they are related to the depth of visual deficits found in amblyopia.

Acknowledgements

Above all, my parents deserve a plentitude of thanks for their everlasting love and support through my journey in life and career. I also have some great friends to thank that have provided encouragement to me during this process.

Thanks to Elise Harb, for devoting so much of her time and knowledge towards this project, and for leading a great example as teacher, advisor, clinician, and researcher.

I also wish to thank Stacey Choi for her time and expertise dedicated to the acquisition of AO images and in lending her advice towards the project and in the analysis involved throughout the duration of this study.

Thanks to Nathan Doble and the members in the AO lab for their assistance with the AO component of this study.

Acknowledgements are also extended to Li Deng for her helpful statistical advice and to the NECO library staff for helping to acquire the many journal articles required for this work.

Table of Contents

Chapter 1: Introduction
- Amblyopia……..……1
- Effects of Amblyopia on the Visual Pathway……..……2
- Investigation of Retinal Function in Amblyopia…….…….4
- Retinal Development and Potential Alteration in Amblyopia…….….5
- Functional Deficits in Amblyopia……6
- Use of Optical Coherence Tomography (OCT) to Study Amblyopia……..7
- Adaptive Optics Imaging……..8
- Study Aims……...…...…….9

Chapter 2: Methods
- Subjects……11
- Clinical Tests of Visual Function & Treatment History Questionnaire……..11
- Imaging……15
- Data Analysis..……21
- Statistical Analysis..……24

Chapter 3: Results
- Subject Characteristics…….....26
- OCT Scanning……..28
- Effect of Axial Length on OCT Measurements…….……..36
- Adaptive Optics (AO) Imaging……..……..38

Chapter 4: Discussion
- Retinal Nerve Fiber Layer Thickness (RNFLT) ……47
- Macular Thickness……...48
- Adaptive Optics (AO) Imaging…….…...51
- Correlation to Visual Function…….……53
- Limitations……...54
- Future Work…….....55
- Conclusions……..56

Bibliography……....57

Addendum
- Questionnaire for Potential Amblyopic Subjects…….....63

List of Figures and Tables

Figure 1. Ocular Dominance in Visual Cortex……..3
Figure 2. Retinal Organization……...4
Figure 3. PSF Correction with Adaptive Optics……9
Figure 4. Retinal Layer Segmentation of Horizontal OCT Scan…….17
Figure 5. NECO AO Fundus Imaging System…….20
Figure 6. Correlation of Axial Length to Refractive Error……..27
Figure 7. Global and Quadrant RNFLT……...29
Figure 8. Mean IRT……..30
Figure 9. Individual IRT……..31
Figure 10. Mean ORT……..34
Figure 11. Individual ORT……...35
Figure 12. Retinal Thickness Measurements and Axial Length……..37
Figure 13. Cone Density Comparison……..39
Figure 14. Mean Cone Density of Subject Groups by Retinal Position……..42
Figure 15. Cone Selection and Voronoi Analysis……43
Figure 16. Voronoi Analysis at 4-degree Temporal Retina…….44
Figure 17. Voronoi Analysis in Amblyopic Subject A7……..45
Figure 18. Voronoi Analysis at 2-degree Temporal Retina…….46

Table 1. OCT Studies in Amblyopia…….8
Table 2. Clinical Characteristics of all Subjects……..13
Table 3. Tests of Visual Function……15
Table 4. Mean RNFLT Among Subject Groups……..30
Table 5. ORT by Subject Group ……33
Table 6. Subject Group Cone Density …...…….40

Introduction

Amblyopia

The defining functional loss in amblyopia is decreased visual acuity in the amblyopic eye in the absence of structural or pathologic abnormalities and in the presence of one of the following amblyogenic factors before the age of six: 1) constant unilateral strabismus, 2) amblyogenic anisometropia, 3) amblyogenic bilateral isometropia, 4) amblyogenic uni- or bilateral astigmatism, or 5) image degradation.[1] Ciuffreda et al. suggest the following clinical classifications for amblyopia: strabismic, anisometropic, isoametropic, and image degradation.[2] Reports of the prevalence of amblyopia in schoolchildren range from 0.7 to <3%.[3–7] Furthermore, in the under-60 age group, amblyopia is the leading cause of unilateral visual impairment in some populations in the United States.[8,9] The risk of vision loss in the better seeing eye in people with amblyopia has been reported to be 3 times compared to the general population.[10]

Annual vision screenings are recommended in the pediatric, primarily preschooler aged (3-5 years) population to identify potential amblyogenic risk factors, with pre-determined pass/refer guidelines in order to maximize the early identification of children at risk for developing amblyopia.[11] Screening guidelines in the state of Massachusetts, for example, require that a vision screening is performed prior to a child's entrance in kindergarten, or performed within the first 12 months within the school, if the initial requirement is not met. Testing performed in the preschool age group includes linear

distance visual acuity and testing of stereopsis and ocular alignment with Random Dot E test.[12]

Treatment for amblyopia includes early spectacle correction, either alone or in conjunction with occlusion therapy either via patching or by pharmacological treatment with atropine.[13] Studies have shown that the best response to treatment occurs in children below the age of 7; however, improvement of visual acuity has been demonstrated in older age groups, especially in the absence of prior treatment.[14,15]

Effects of Amblyopia on the Visual Pathway

Classically, the explanation for visual loss from amblyopia is found within the primary visual cortex. In animal models of deprivation amblyopia by lid suture, Hubel and Wiesel found the ocular dominance columns of the primary visual cortex to be shifted in cats subjected to unilateral lid suture.[16] In this paradigm, the shift in ocular dominance columns demonstrated a decreased responsiveness of the cells in the primary visual cortex (V1) that normally received input from the deprived eye. Thus, the abnormal visual experience caused an alteration (reduction) in the cortical response to the deprived eye, replaced by a stronger response to the dominant (non-deprived) eye. This concept is illustrated in Figure 1, which shows a diagram of the altered cortical response in both monocular and binocular cells in the experimental cases of unilateral lid suture.[17]

It is likely that the time in which an amblyogenic factor first presents itself will determine which part of the visual system is altered. The developmental window for neural plasticity, known as the critical period, for layer IV of the primary visual cortex has been

shown to end sooner than the critical period for development of dominance in layers II, III, V, and VI, in experimental cat models.[18] This hypothesis has been supported in humans by a post-mortem study of an anisometropic amblyope that did not display a change in ocular dominance columns in layer IV of the striate cortex (V1). In this case, it is hypothesized that anisometropia was likely established after maturation of layer IV of the striate cortex.[19] Another study found normal striate (V1) function but abnormal extrastriate (V2-V5), higher visual cortical area, function in strabismic human amblyopes in positron emission tomography (PET) scan studies.[20] Thus, there is evidence that different cortical sites are affected depending on the time scale and type of interruption on development of the visual system.

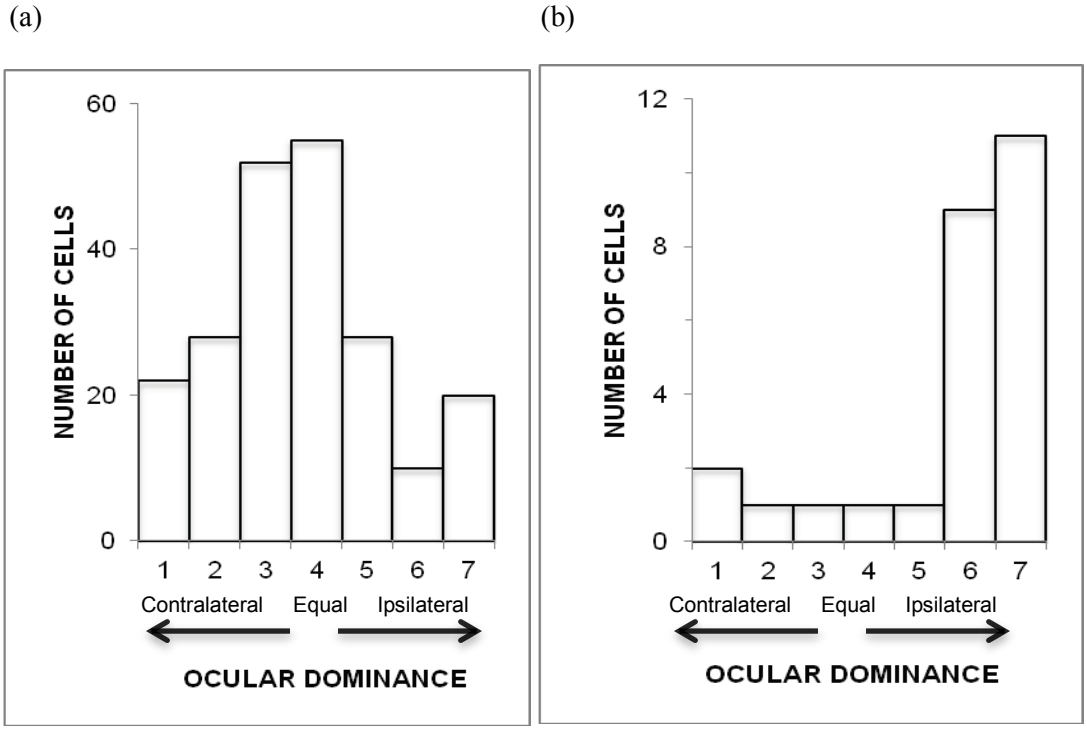


Figure 1. Ocular Dominance in Visual Cortex. Graphs illustrating sampling of cortical cells responding monocularly or binocularly from (a) kitten reared with normal vision and (b) kitten reared with lid suture at the age of 9 weeks. Adapted from Wiesel & Hubel, 1963[16]

Change in the lateral geniculate nucleus has been also investigated in amblyopia. Cell shrinkage in ipsilateral lateral geniculate nucleate cells in layers receiving input from the amblyopic eye has been noted in human strabismic amblyopia, as well as the macaque monkey strabismic model[21] and the kitten form deprivation model.[16]

Investigation of Retinal Function in Amblyopia

The retina is considered to be neural tissue, since it forms as an invagination of the diencephalon, known as the optic vesicle.[22] In the simplest course, two basic synapses occur within the retina in response to light before synapse occurs in the lateral geniculate nucleus: photoreceptor cell to bipolar cell, and bipolar to retinal ganglion cell (see Figure 2).[23]

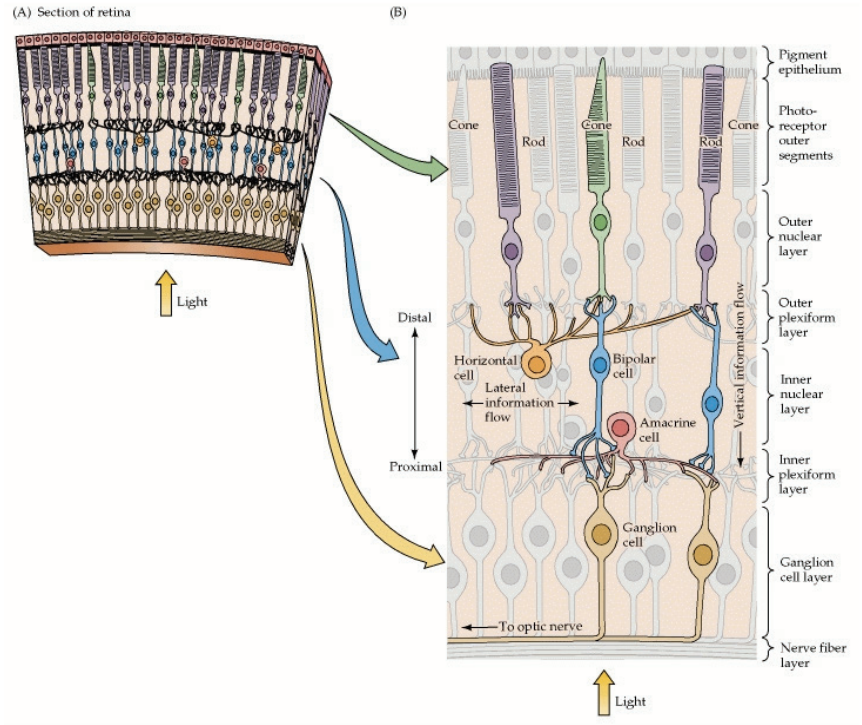


Figure 2. Retinal Organization. The retina is organized in layers of cells and their axons, with the direction of light shown in (a) from anterior to posterior retina. (b) shows cell bodies and their axons that make up the layers of the retina. Image obtained from Purves, et. al[22]

For its role in the visual pathway and as part of the neural visual system, basic retinal function has also been investigated for its susceptibility to the pathology of amblyopia. It has been debated whether the functional markers of the retina, such as the pattern electroretinogram (ERG) and the Stiles-Crawford effect (SCE) of the amblyopic eye is abnormal.[24–28] The SCE measured by psychophysical technique was found to be flatter in eyes with amblyopia[29,30] while a more recent study using a double pass technique showed unaffected SCE in amblyopia.[28]

Retinal Development and Potential Alteration in Amblyopia

Two main events occur in the development of the fovea: 1) the outward migration of the inner retinal layers to form the foveal pit, and 2) cone packing into the central foveal area. This process occurs during early infancy, and reaches maturity between 15 and 45 months of age.[31] Yen et. al. have suggested the arrest of the normal apoptosis of retinal ganglion cells (RGCs) as a possible cause of the thicker nerve fiber layers observed in amblyopes.[32] However, in experimentally deprived eyes, the normal process of apoptosis still occurs in the deprived eye, yet is shown to result in an increased number of RGC's in the untreated (non-deprived) eye.[33] Complete arrest of action potentials has been shown to affect the mosaic regularity of a sub-set of RGCs in one study.[34] Animal models of deprivation amblyopia by dark rearing or lid suture have also reported changes in retinal layers.[35–37] The application of these studies to human cases, however, may not be straightforward, as human amblyopia most commonly occurs by strabismus or refractive causes, not complete deprivation.

In some studies, the physical characteristics of the optic nerve in amblyopic subjects have also been implicated as the etiology of some vision loss. The presence of segmental dysplasia[38] and reduced retinal rim area[39] have been proposed as underlying anatomic factors leading to a clinical picture of amblyopia in studies using fundus photographs. However, more recent studies using HRT to investigate disc parameters found no difference between amblyopic and fellow eye optic nerve parameters.[40] Other structural analyses suggest that the fellow eye, like the amblyopic eye, shows anatomic differences as compared to control groups of eyes,[41,42] but do not differ enough to be clinically significant.[42]

Regardless of the hypothesized retinal alterations possible from amblyopia, the conversation is further complicated since the classical assumption that amblyogenic risk factors such as strabismus and anisometropia precede amblyopic visual deficits has also been brought into question.[43]

Functional Deficits in Amblyopia

Diminished foveal function has been reported in both treated amblyopic and fellow eyes when compared to control eyes using rarebit VA testing, a perimetric testing technique using bright targets smaller than receptive field size presented in the fovea. No difference was found between function in amblyopic eyes when compared to fellow eyes using this testing technique, however.[44]

Accommodative behavior has also been shown to be decreased in amblyopes,[45,46] which has been shown to improve, but not completely recover to normal function, after treatment.[46]

The relationship between the cause of the amblyopia and visual function has also been explored. Anisometropes, strabismics, and strabismic anisometropes (mixed amblyopes) behave differently on various acuity tasks and contrast sensitivity measures. In addition, binocularity has a large effect on visual function: non-binocular observers tend to have poorer optotype and Vernier acuity,[47] and strabismic anisometropes tend to have the poorest outcomes on these acuity tasks.[48]

Use of Optical Coherence Tomography (OCT) to Study Amblyopia

Sophisticated imaging techniques are needed to determine anatomical differences of the retina *in vivo.* Thus far, OCT has been utilized to examine thickness variations of the retinal layers in amblyopes. OCT technology provides the ability to take in-vivo cross-sectional images of the human retina, and Fourier Domain technology, in particular, provides increased axial resolution (typically 5 μm) of these images.

Using OCT technology, retinal thickness parameters, typically macular thickness[49–54] and RNFL thickness[32,49,52,54–57] in amblyopia have been compared to their fellow, and more rarely, non-amblyopic control eyes. However, the results of these studies are conflicting in determining whether there is a difference in the retina, as measured via thickness of retinal layers using OCT, of the amblyopic eye. Many studies investigating macular thickness report either no significant difference[49,54] or an increased[50–53] macular thickness in amblyopic eyes. Furthermore, some studies report macular thickness changes only in anisometropic[53] or strabismic[51] amblyopic sub-groups. In a novel analysis, Park et. al. investigated retinal thickness surrounding the macula, but at different eccentricities and included sub-layer

analysis, finding less thickness within the ganglion cell layer/inner plexiform layer (GCL/IPL) in amblyopic subjects.[58] For a summary of these studies and their findings refer to Table 1. However, direct comparison of results between these studies is not always possible due to differences in OCT instrumentation used, variations in definitions of amblyopia within subject groups, and the use of either a separate control group or the fellow eye as control.

Author	Subjects	Main Findings
Yen (2004)	n=40 (strab/aniso)	↑ RNFLT
Altintas (2005)	n=14 (strab)	No diff in RNFLT
Yoon (2005)	n=31 (aniso) 5-12y	↑ RNFLT, no diff in MT
Kee (2006)	n=26 (all types) ~8y	No diff in MT or RNFLT
Repka (2009)	n=37 (all types) 7-12y	No diff in RNFLT
Huynh (2009)	n=65 (all types)	↑MT
Dickmann (2009)	n=40 (strab/aniso)	↑MT in strabs
Aguirre (2010)	n=124 (mild vs severe) 4-10y	↑ RNFLT, ↑MT in slight ambly
Al-Haddad (2010)	n=45 (strab/aniso)	↑MT in aniso, no diff in RNFLT
Miki (2010)	n=50 (perisistent vs recovered)	No diff in RNFLT
Park (2011)	n=20 (strab/ptosis/cyl)	↓GCL/IPL

Table 1. OCT studies in amblyopia.

Adaptive Optics Imaging

Adaptive optics (AO) imaging technology was originally introduced for application in astronomical imaging.[59] The use of AO in ophthalmic applications makes it possible to acquire ultrahigh resolution *in vivo* retinal images at the cellular level. Without a correction of the higher order aberrations of the eye, imaging resolution is limited. Such high-resolution images are possible through a dynamic correction of the eye's high order aberrations in real time. A Hartman Shack wavefront sensor is used to measure the aberration profile of light emerging from the eye, which is, in turn, corrected by a deformable mirror (DM). Figure 3

shows the performance of the AO fundus camera used in this study: the point-spread function (PSF) is improved to a diffraction-limited resolution by this process. An overview of the technical aspects involved in AO imaging for ophthalmic purposes is provided by Doble.[59] The use of AO imaging has been used to investigate various retinal conditions at the cellular level, such as retinal dystrophy,[60,61] glaucoma,[62] optic neuropathies,[63] and axial myopia.[64] Furthermore, images obtained through this technology have been used to make comparisons between the characteristics of the cone mosaic and visual function.[61]

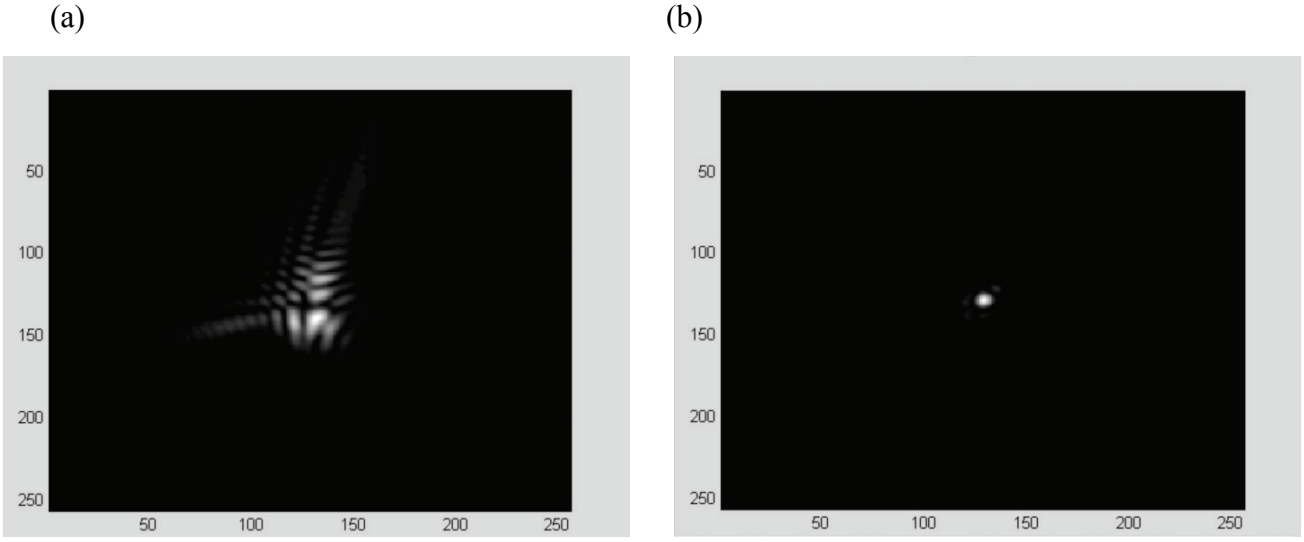


Figure 3. PSF Correction with Adaptive Optics. Example of point spread function of subject C1 before AO-correction (a), and after correction (b) during imaging.

Study Aims

The aim of this study is to investigate potential retinal differences in the eyes of amblyopic subjects through the use of two non-invasive imaging modalities. OCT imaging allows the evaluation of the thickness of specific inner and outer retinal layers in the macular

and peri-papillary areas, while AO fundus imaging allows the analysis of cone photoreceptor density and their packing arrangement in specific areas of the retina. Differences will be compared between amblyopic eyes, fellow eyes, and control eyes. Studying the same macular areas, 2- and 4- degree nasal and temporal eccentricities from the fovea, with these two imaging techniques allows potential correlates to be made if any differences are observed.

Methods

Subjects

Subjects were recruited from the student population of The New England College of Optometry (NECO) in accordance with the Declaration of Helsinki and under the approval of the Institutional Review Board of NECO. Informed written consent was acquired prior to testing. Inclusion criteria for amblyopic subjects included (1) a self-reported history of amblyopia (treated or un-treated) caused by an amblyogenic refractive error and/or strabismus, (2) best corrected visual acuity of 20/20 or better in the normal eye, and (3) a non-cycloplegic refractive error of ± 8.00D spherical equivalent with astigmatism less than -2.00D. The specific methods used to determine these criteria are described in detail below. Inclusion criteria for control subjects included (1) visual acuity of 20/20 or better in both eyes and (2) the presence of a minimal non-cycloplegic refractive error (between -0.25D and +1.00D). Exclusion criteria for all subjects included either a history of eye injury or surgery including refractive surgery, presence of cataract or other media opacity, and/or ocular disease.

Clinical Tests of Visual Function & Treatment History Questionnaire

All subjects recruited in the study first underwent basic clinical testing to determine eligibility and their clinical characteristics. Best-corrected visual acuity was determined

using a calibrated computerized visual acuity system (Precision Vision Acuity Testing, Chicago, IL, Version 4.0), placed 13-feet away. The computerized visual acuity system has the ability to display randomized Sloan letters on a LogMAR scale. Since amblyopes classically have lower visual acuity performance under crowded conditions,[65,66] several considerations were made to ensure that the visual acuity test appropriately quantified the vision of both amblyopic and normal subjects. First, a 'gold-standard' Sloan letter whole chart visual acuity test utilizing LogMAR spacing was used. Second, to ensure equal crowding within a line of letters, seven letters were presented in each line instead of the typical clinical presentation of five letters. However, the two outer letters were not scored for acuity measurements, since they have only one neighboring letter and potentially could be easier to 'see' by amblyopes.

Visual acuity testing started at the 20/80 Snellen equivalent line (0.6 LogMAR) and all subjects were encouraged to read the next smaller line, until the subject was incorrect for the majority of the line. Given that the visual acuity chart used utilized a LogMAR scale, the total number of correct letters was calculated for each subject and converted into a LogMAR visual acuity. That is to say, each 'correct' letter scored was assigned a value of 0.02, the product of which was subtracted from 0.70 (the value for total possible correct). For reference, the scaling of LogMAR acuity is such that a LogMAR value of 0.0 is a 20/20 Snellen visual acuity equivalent.

The formula used for the calculation of LogMAR visual acuity in this study was:

LogMAR acuity = 0.7 – (0.02 X (total number of letters correct))

Subject	Age	Sex	RE (SE)	LogMAR VA	Strabismus?	Monofixation syndrome?
C1	25	M	R: +1.375	-0.20	No	No
			L: +1.375	-0.26		
C2	22	F	R: +1.00	-0.18	No	No
			L: +1.00	-0.16		
C3	24	F	R: -0.50*	+0.02	No	No
			L: pl*	-0.08		
C4	24	F	R: -0.25*	-0.06	No	No
			L: -0.12*	-0.18		
A1	27	F	R: +4.375	-0.12	LET D&N	OS
			L: +3.75	+0.24		
A2	25	M	R: +5.625	-0.08	RET D&N	OD
			L: +5.00	-0.14		
A3	25	F	R: +5.50*	-0.10	Alt ET D&N (cc)	OS
			L: +5.75*	-0.08		
A4	23	F	R: +4.50	-0.18	Ortho (cc) D&N LET (sc)	OS
			L: +5.00	+0.02		
A5	24	F	R: +2.25	-0.08	L(ET) 60% @ N	OS
			L: +2.25	+0.06		
A6	24	F	R: +0.75	-0.14	No	OS
			L: +4.50	+0.26		
A7	23	F	R: +1.50	0.00	No	No
			L: +5.50	0.00		

*Refractions in asterisks not obtained by cycloplegic auto-refraction.

Table 2. Clinical Characteristics of all Subjects. Monofixation syndrome defined as presence of either eccentric fixation and/or central suppression as demonstrated in clinical tests described previously.

If visual acuity in an amblyopic eye was initially worse than 20/20 with the subject's habitual prescription, subjective refraction was performed and best-corrected visual acuity was re-tested. Subject refractive error was determined by open field autorefraction (Grand Seiko WR-5100K) both under non-cycloplegia (for the purposes of subject screening) and under cylcoplegia prior to AO imaging (all but n=2 control subjects and n=1 amblyopic subject; see Table 2). Cycloplegic auto-refraction was measured 30 minutes after the instillation of a second drop of 1% cyclopentolate, and prior to imaging with an AO fundus

camera, as discussed below. Subjects' habitual correction was obtained either by lensometry and/or contact lens prescription information.

All subjects underwent clinical testing to evaluate and quantify their visual function. Specifically, color vision was tested using the HRR #6 test booklet to rule out any cone photoreceptor abnormalities that are caused by conditions other than amblyopia. Stereoscopic acuity was tested using Random Dot E cards at a testing distance of 5 feet, with a pass cut-off of three out of five correct. Distance and near cover tests were performed to evaluate for any strabismus, with a supra-acuity letter target for both distances. Visuoscopy, traditionally used to measure and quantify eccentric fixation, was performed by placing a grid target on the retina with a direct ophthalmoscope and noting the location of the foveal reflex with respect to the grid pattern projected on the retina. The 4Δ Base Out test was used to determine if subjects had central suppression; if suppression was suspected, a walk away distance Worth 4 Dot testing technique was used to confirm the findings. The Worth 4 Dot technique is performed by initially asking the subject to describe what dots are seen at near (using peripheral fusion). A presumed fusion response would be a report of seeing 4 dots. Then, the examiner slowly walks away while continuing to show the subject the Worth 4 Dot flashlight and asking subjects to describe if any changes in their perception of the projected four dots occur. If at any point the subject reports the disappearance of either eye-specific dot target, indicating a central suppression response, the findings concur with the 4Δ Base Out test. See Table 3 for a summary of clinical tests performed in the study.

Testing Category	Testing Method
Visual acuity	PVAT computer system
Ocular alignment	Cover test at D & N with habitual correction
Color vision	HRR#4
Stereoacuity	Random Dot E
Eccentric fixation	Visuoscopy
Central suppression	4Δ base out testing

Table 3. Tests of Visual Function. Testing performed in this study to evaluate visual function of all subjects.

In order to better classify the type, duration, and success of treatment in the amblyopic subjects recruited in this study, all amblyopic subjects answered a questionnaire verbally administered by an examiner. The questionnaire probed what kind of treatment was initiated, the onset and duration of treatment, and history of compliance. If any strabismus was present, questions about awareness and control of strabismus was also probed (see Addendum 1).

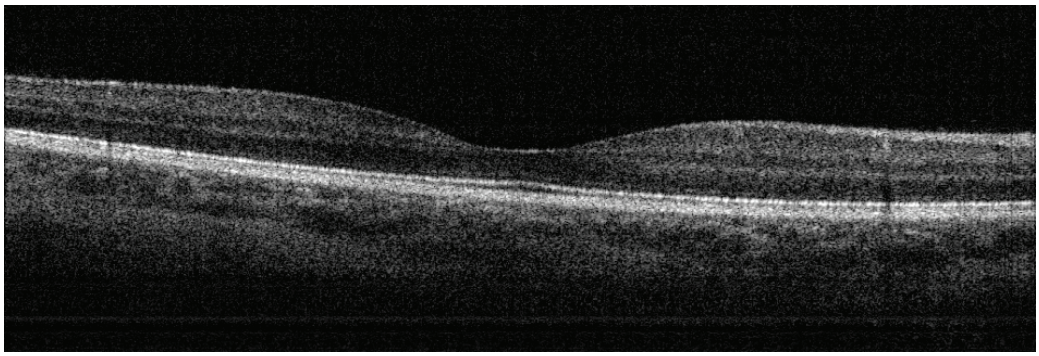
Imaging

A Spectral Domain Optical Coherence Tomography (SD-OCT) (RTVue, Model RT-100, Optovue, Inc. Fremont, CA) was used to obtain cross-sectional retinal images of all subjects. It acquires 26,000 A-scans/second with a depth resolution of 5 μm using a scanning laser diode at a wavelength of 840±10 nm. In addition, the RTVue has an 'auto-all focus'

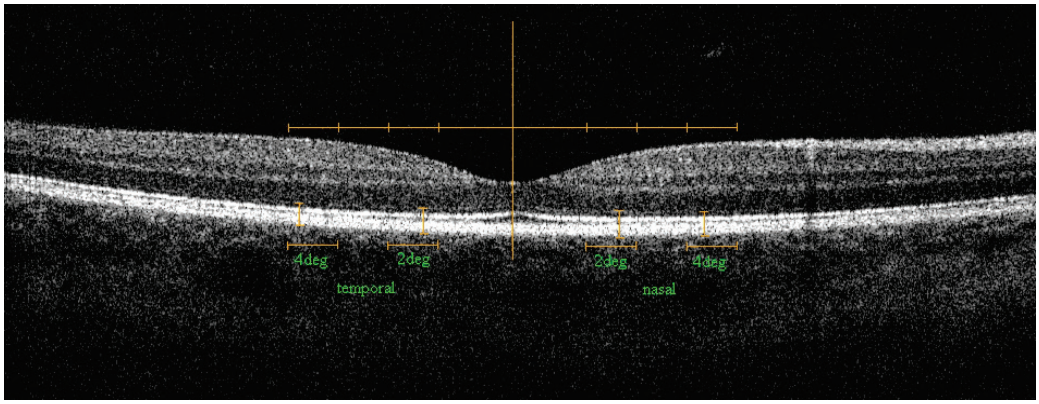
feature, which was utilized in an attempt to diminish any retinal magnification effects that might have occurred due to differences in subjects' axial lengths. This feature automatically estimates the subject's refraction, in diopters, and accordingly adjusts the system's configuration to minimize magnification errors. All OCT testing was performed in dim room illumination and on natural pupils (>3mm), testing the right eye first. All scans were inspected for good image quality (SSI score must be greater than 50, and image must have no shearing).

To investigate macular thickness, two different macular scans were performed. First, a registration SLO scan (3D Macula) was taken to provide baseline data in the RTVue program for subsequent macular scans. Following this scan, several macular scans were obtained using the MM6 scan design (a circular scan 6mm in diameter consisting of 12 radial line scans through the central fixation point). Each scan was performed three times per eye. A representative retinal cross section from one of the radial scans is shown in Figure 4a. For each scan, the average total retinal macular thickness is computed by the OCT software in microns for the central 1.0 mm area of the fovea and for each of the ETDRS quadrants (nasal, temporal, superior, and inferior) of the para-fovea (inner 1.0 - 3.0 mm ring) and peri-fovea (outer 3.0 - 5.0 mm ring) for a total of 9 regions.

(a)



(b)



(c)

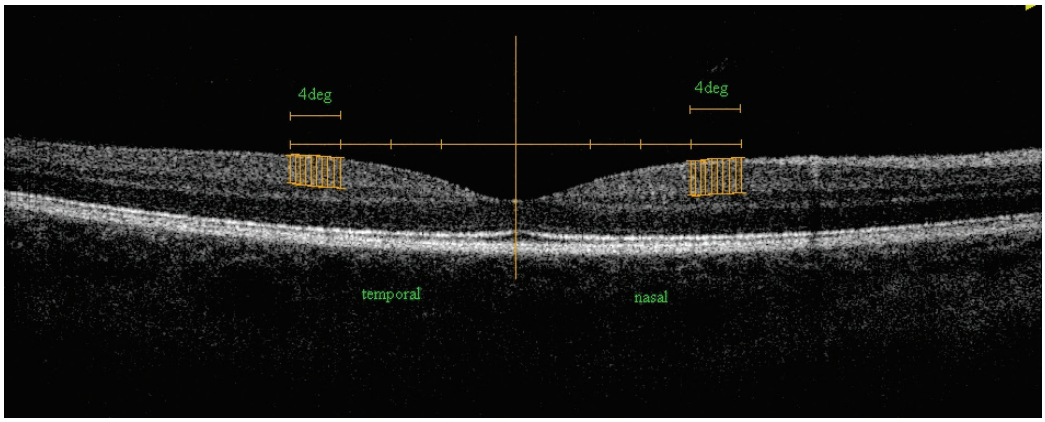


Figure 4. Retinal Layer Segmentation of Horizontal OCT Scans. (a): Black and white cross-section of retina by OCT, (b): example of outer retinal layers (ELM to RPE/choriocapillaris interface) selected at 2- and 4- degree nasal and temporal eccentricities from the foveal center. (c): example of inner retinal layers (ILM to IPL/INL interface) selected at 4- degree nasal and temporal eccentricities

Following the macular scans, optic nerve head (ONH) scans were taken to measure retinal nerve fiber layer thickness (RNFLT). First, a registration SLO scan (3D Disc) was taken, which is used for registration of subsequent ONH scans. The automated fixation target for all optic nerve scans was 20° nasal from straight ahead; the examiner selected the center of the disc during imaging by viewing a live video of the fundus. Following the registration scan, three ONH scans were taken (a 5mm diameter circular scan around the ONH). The RTVue OCT software automatically draws the optic disc borders, but the examiner also visually inspected the disc border drawings for possible errors. RNFLT determined from each ONH scan is reported globally and by quadrant.

Some of the subjects (C1-C4 and A1, A5-A7) were also imaged with a Flood-Illuminated AO- Fundus camera. Unfortunately, due to subject time constraints and/or declining cycloplegia due to side effects, not all subjects were able to participate in AO fundus imaging. Prior to AO imaging, baseline eligibility for dilation was determined for each subject. Intraocular pressure was checked with a non-contact tonometer (NCT) and the anterior chamber angle examined using the Van Herrick technique. If the subject was deemed safe to be dilated, two drops of 1% cyclopentolate hydrochloride ophthalmic solution, separated in administration by 5 minutes, and one drop of 2.5% phenylepherine hydrochloride ophthalmic solution were used. The AO imaging was then performed at least 30 minutes after the dilating drops were instilled. Cycloplegic conditions were imperative for imaging, as accommodative fluctuations would influence the power of the eye and degrade image quality during imaging.

The axial length of all subjects was measured using the Zeiss IOL Master (version 3.02, Carl Zeiss Meditec, Jena, Germany) to calculate the scaling factor attributed to the size of the subjects' eye. The scaling factor was used to convert degrees to microns on the retina for cone density calculation and for lateral area calculations within OCT images. At least four axial length measurements were taken per eye, with the right eye always tested first. Several factors for each measure were inspected to ensure optimal measurement quality and low variability. First, each measure was checked to verify that the SNR (signal-to-noise ratio) value was greater than 2.0. Second, all axial length measurements for a given eye had to agree within 0.02 mm. If this criterion was not satisfied, then additional measures were taken until the variability of measures was within 0.02mm. Finally, resulting waveforms were checked to ensure the axial length waveform (a measure of time-based quality of light reflection) did not have a double peak, indicating a poor quality scan. Once all criteria were satisfied, the average axial length value was used for all future analyses.

To minimize head movements during AO imaging, a bite bar was prepared using dental impression putty for each subject. Subjects were instructed to view the tip of a small arrow placed on a fixation target (bull's eye pattern subtending a ~12° diameter of visual angle). Imaging locations were at 2- and 4- degree eccentricities from the fovea, both in the nasal and temporal directions. Only the right eye of control subjects was imaged, whereas both eyes of amblyopic subjects (amblyopic and fellow eyes) were imaged. Ocular aberrations were measured by a Hartmann-Shack wavefront sensor and corrected by a microelectromechanical systems (MEMS) deformable mirror (DM) (37 segment, Iris AO, Inc). See Figure 5 for a representative image of the NECO AO fundus imaging system.

Subjects' refractive error was corrected with trial lenses prior to AO imaging. AO images were taken when the ocular aberrations were corrected down to an adequate level, typically to about 0.08-0.10 microns, with 10 ms exposure at 650 nm imaging wavelength. Multiple images were taken at each retinal location, until approximately 7-10 good images were obtained.

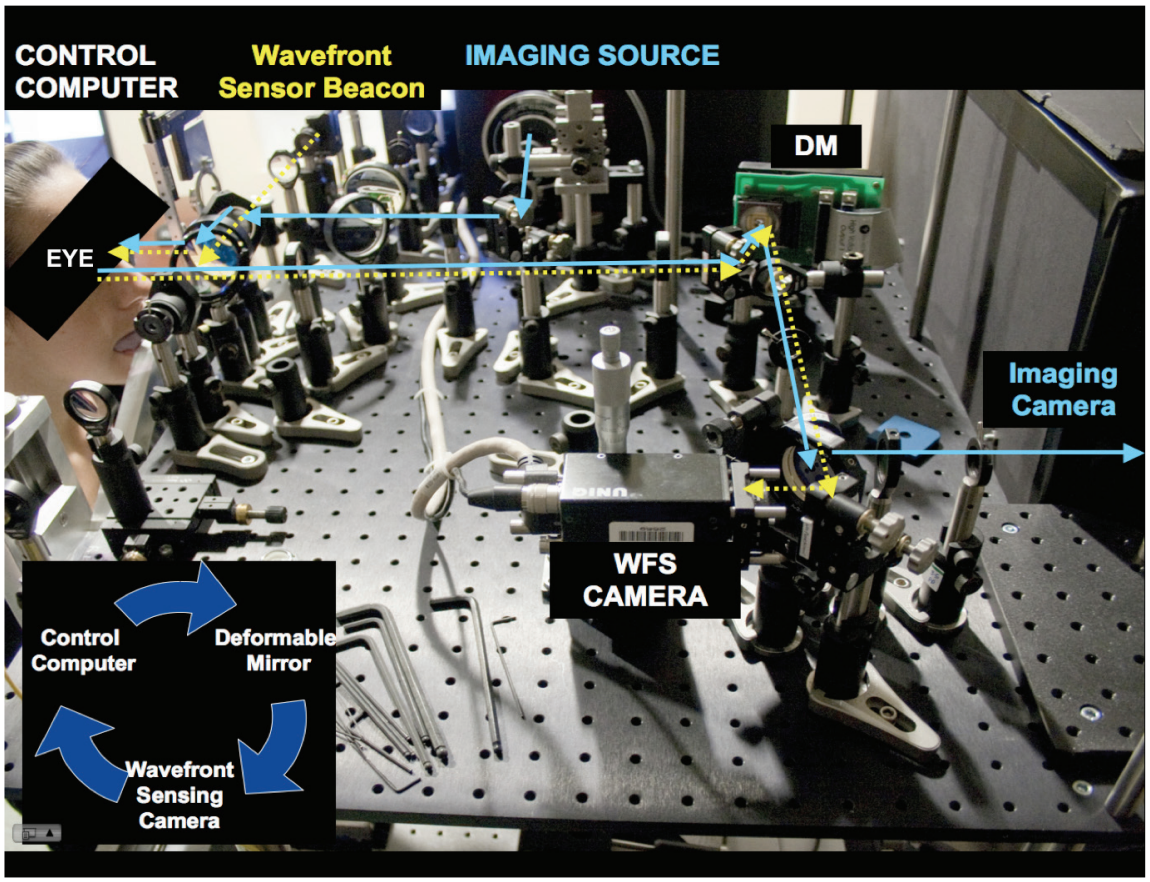


Figure 5. NECO AO Fundus Imaging System. Blue arrows show path of imaging light, while dotted arrows show path of SLD beam measuring real-time aberrations of imaging system.

Data Analysis

OCT Analysis

Retinal Nerve Fiber Layer Thickness (RNFLT) values were output from the RTVue OCT software program directly. The Optovue system generates average thickness values for nerve fiber layer thickness surrounding the optic nerve head, as both a global average and by each quadrant: superior, inferior, nasal, and temporal.

To investigate if potential changes were specific to a particular retinal layer, retinal thickness in the macular region was evaluated in the context of its inner and outer retinal layers. From the cross-sectional macular scans, specific retinal layers were selected to determine the thickness of the outer (ELM to RPE/choriocapillaris interface) and inner (ILM to IPL/INL interface) retinal areas, separately, as described below.

Outer Retinal Thickness (ORT) was estimated from each OCT MM6 scan by selecting a one degree lateral area of the horizontal scan (180-degree meridian), surrounding 2- and 4- degree eccentricities nasally and temporally from the foveola. The above ORT analysis was performed to compare thickness values to photoreceptor density determined at the same retinal positions investigated with AO imaging. All 2- and 4- degree position locations in the scan were estimated by using each subject's axial length to calculate lateral distance per degree, using the formula:

$$x = 1000 * [(AL\ (mm)/1.37) * \tan(3.142/180)]$$

where x = diameter of 1 degree retinal patch in microns, AL=axial length in mm, and the expression (AL/1.37) is the calculation for the focal length of the eye.

Using the digital caliper tool in the RTVue OCT software, the examiner visualized the external limiting membrane (ELM) and retinal pigment epithelium (RPE)/choriocapillaris interface[67] and took thickness measures between the two layers to segment the ORT (see Figure 4b). For each scan, this measure was repeated ten times within each 1-degree lateral area to reduce measurement variability. The ten values were then averaged to determine the location's retinal thickness. This procedure was then repeated for all three macular scans and the values were averaged to create a mean retinal thickness for each retinal location. These mean values were used for all subsequent ORT data analysis. This digital caliper technique was used in order to specifically select the outer retina from the ELM to RPE, as the OCT software defines the outer retinal thickness from the outer nuclear layer to RPE by default. The same examiner performed all measurements.

Inner retinal thickness (IRT) is defined in this study as the distance from the innermost border of the retina, the inner limiting membrane (ILM), to the interface between the inner plexiform layer (IPL) and inner nuclear layer (INL), thus including the IPL (see Figure 4c). This section of the retina was selected due to its potential to have correlations with RNFLT, and because it contains the final synaptic neural connection within the retina within the IPL. IRT was measured from each horizontal (180-degree meridian) scan by caliper measurement in an identical way as described for ORT measurement. Ten

measurements within a one degree lateral area at four degrees nasal and temporal from the macula were made in each MM6 scan. IRT was only determined at the four-degree eccentricity due to the influence of the foveal pit slope on thickness values of the inner retinal layers at the two-degree position. This process was performed on all three scans and averaged, as described above for the ORT, for all subsequent data analysis.

Thickness measurements using OCT, including RNFLT, IRT and ORT were compared against subjects' axial lengths using a linear regression analysis to evaluate whether there was any correlation between these two measures, since differences in axial length could theoretically cause magnification effects to the OCT images.

AO Image Analysis

Cone density measurements and packing characteristics were calculated using a custom MATLAB (Mathworks, Inc., Natick, MA) software program. First, several best images (range: 2-9 images) from each retinal location were selected based on both subjective judgment and contrast measurements from a custom software program. These images were then registered together to improve image quality by enhancing the signal to noise ratio. The registration program aligns pre-selected images based on cross-correlation of features in the image such as blood vessels and cones. Next, the cone density program locates cones based on threshold values set for minimum cone spacing and dimmest cones. Minimum cone spacing and threshold intensity were manipulated in the program by the examiner to result in the most accurate selection of cones in the image. Cone density (cones/mm^2) was then

calculated by the software program, using the number of cones in the image given the conversion factor for lateral distance per pixel of the image taken for each subject's axial length.

The use of Voronoi diagrams in analyzing photoreceptor arrangement has been described previously;[68] the custom program uses the placement of cones identified in the cone density program and calculates the distance between individual cones and the number of neighboring cones. This allows analysis of deviations away from a hexagonal packing of photoreceptors. The number of cones in each image with a given number of neighboring cones (ranging from 0-11) was documented and illustrated graphically. Cones labeled as having 0 neighbors were as a result of edge artifacts and not included in analysis.

Statistical Analysis

The following statistical tests were used for comparing global and quadrant measures of RNFLT, ORT, and IRT using OCT. Values between amblyopic and control eyes with were compared using unpaired t-test and between amblyopic and fellow eyes using paired t-test, to test for significant differences.

Linear regression was used to evaluate the effect of axial length on various retinal thickness measurements to ensure that there was no effect of magnification on OCT-derived results.

Cone density values obtained via AO imaging were averaged within subject groups. Mean density of amblyopic and fellow eye groups were compared to the control group confidence interval, defined here as the range of mean density ± standard deviation of control eye measurements.

Differences in the proportion of cones with 4-8 neighbors, as determined from Voronoi analysis, were compared between subject groups using ANOVA.

Results

Subject Characteristics

The average age of the amblyopic subjects (n=7) recruited was 24.43 years (range 23-27); the average age of hyperopic control subjects (n=4) was 23.75 years (range 22-25). The average (± s.d.) spherical equivalent refractive error was +4.59D (±1.27) for amblyopic and +3.39D (±1.84) for fellow eyes. The control subjects had an average (± s.d.) spherical equivalent refractive error of +0.58D (±0.75) and +0.64D (±0.70) in their right and left eyes, respectively. The average LogMAR visual acuity for amblyopic eyes (0.06 ± 0.14, range 0.00 to +0.26) was, as expected, worse than the visual acuity for fellow eyes (-0.11 ± 0.06, range -0.18 to 0.00). Also as expected, control eyes had equal and good visual acuity (-0.16 ± 0.07, range -0.26 to 0.02). Mean axial length in amblyopic eyes was slightly shorter (21.90 ± 0.89 mm (range 20.57 to 23.42) than in fellow eyes (22.27 ± 0.87 mm, range 21.17 to 23.43); however, both amblyopic and fellow eyes were shorter than control eyes, which is consistent with the higher amounts of hyperopia seen in amblyopic subjects. Control eyes had a normal axial length of 23.38 ± 0.69 mm, with a range of 22.58 to 24.39.

Analysis by paired t-test did not reveal any significant differences between the axial length in amblyopic and fellow eyes (p=0.16). However, there was a significant difference between the axial lengths of amblyopic and control eyes by unpaired t-test (p=0.002), with amblyopic eyes generally being shorter than control eyes. Similarly, there was also a significant difference between control and fellow eyes (p=0.016), with the fellow eyes of

amblyopes being generally shorter than control eyes. As expected, there was a strong relationship between axial length and spherical equivalent refractive error in this subject group (R^2=0.67), as shown in Figure 6.

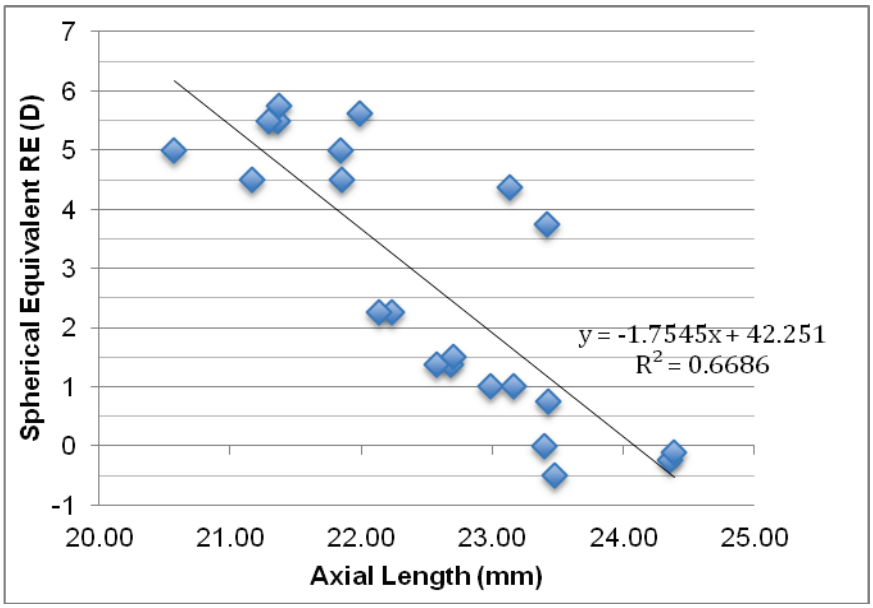


Figure 6. Correlation of Axial Length to Refractive Error. Axial length of all study subjects compared to spherical equivalent refractive error.

All amblyopic subjects had a history of amblyopia treatment with full time spectacle wear and/or patching, except for subject A6, who did not receive a spectacle correction until age 21 years. Subjects A1-A5 demonstrated mixed amblyopia with strabismus in the presence of hyperopia, while the amblyopia of subjects A6 and A7 was purely anisometropic.

See Table 2 for a summary of each subject's ocular characteristics including their outcomes of clinical testing.

OCT Scanning

Out of all OCT scans obtained of the macula and optic nerve, only one macular MM6 scan from subject C2 was not used for analysis due to its signal strength falling below the minimum required level of 50 (out of a possible 100). All other scans (MM6 and ONH) collected were used for data analysis, resulting in three scans per eye of every remaining subject for each scan protocol.

Retinal Nerve Fiber Layer Thickness (RNFLT)

Overall, global RNFLT did not significantly differ between fellow and amblyopic eyes (mean difference, Fellow-Amblyopic, 0.49 μm, $p=0.86$, paired t-test). There was also no significant difference in RNFLT in any given quadrant between amblyopic and fellow eyes (all $p>0.10$, paired t-test), as illustrated in Figure 7a. Likewise, global RNFLT did not differ significantly between control and amblyopic eyes, although amblyopic eyes had slightly thicker RNFLT than control eyes (mean difference, 4.69 μm, $p=0.455$) Likewise, comparisons between amblyopic and control eyes using unpaired t-testing revealed no significant differences in either global or quadrant RNFLT (all $p>0.1$), as demonstrated in Figure 7b. Table 4 summarizes the RNFLT results for subject groups globally and by quadrant.

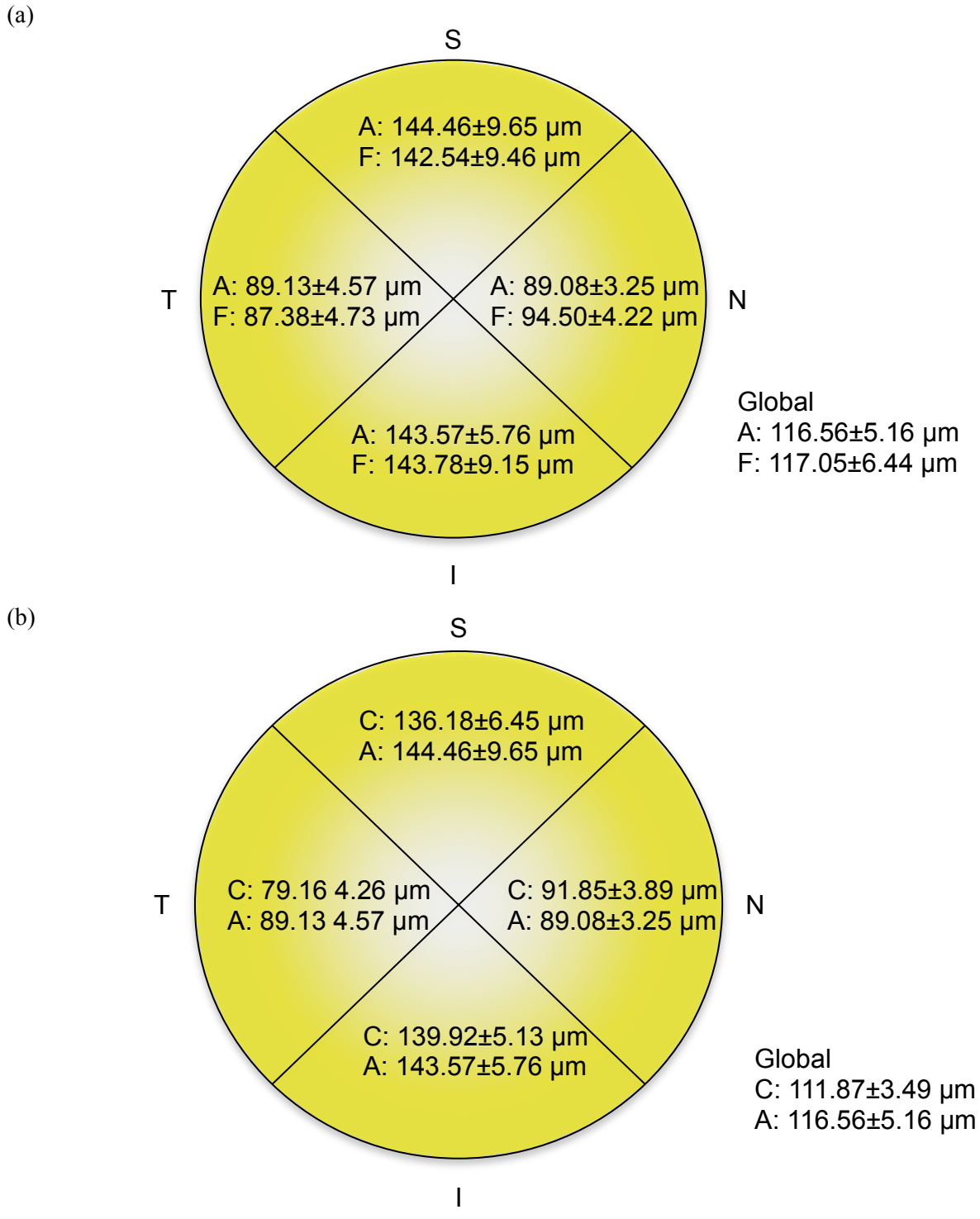


Figure 7. Global and Quadrant RNFLT. Mean RNFLT of (a) amblyopic (A) and fellow (F) eyes; and (b) control (C) and amblyopic (A) eyes.

	Global	Superior	Nasal	Inferior	Temporal
Control	111.87 ± 3.49	117.05 ± 6.44	91.85 ± 3.89	139.92 ± 5.13	79.16 ± 4.26
Amblyopic	116.56 ± 5.16	144.46 ± 9.65	89.08 ± 3.25	143.57 ± 5.76	89.13 ± 4.57
Fellow	117.05 ± 6.44	142.54 ± 9.46	94.50 ± 4.22	143.78 ± 9.15	87.38 ± 4.73

Table 4. Mean RNFLT Among Subject Groups, in μm ± σ

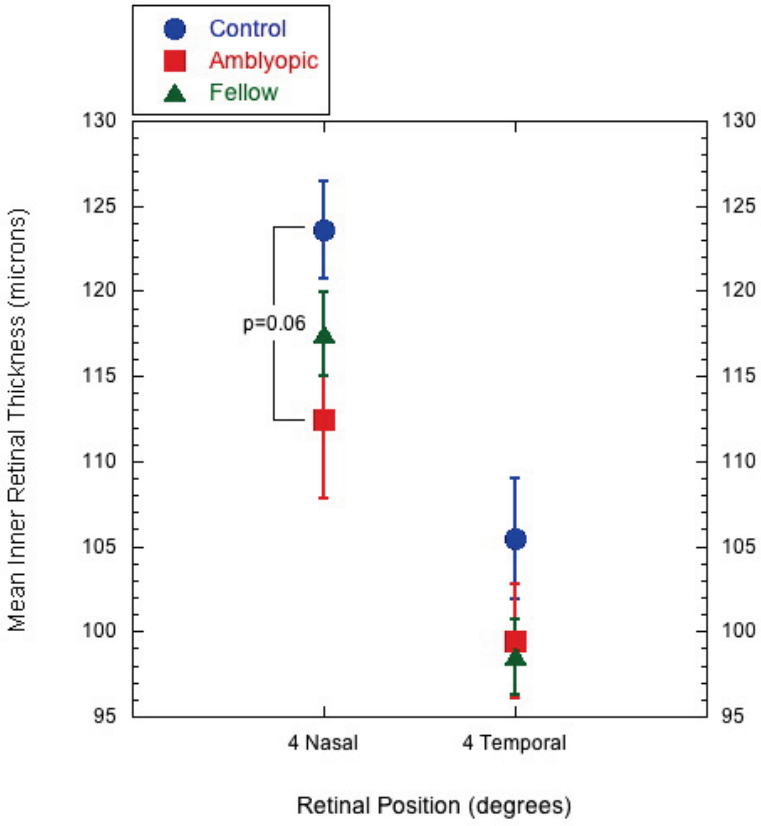


Figure 8. Mean IRT. Subject group mean IRT at the 4- degree nasal and temporal eccentricities

Inner Retinal Thickness (IRT)

Figure 8 shows the average values for inner retinal thickness among each subject group at the nasal and temporal locations. Average IRT at the 4-degree temporal position (Figure 9a) was slightly thinner in both amblyopic (mean 99.42 ± 8.91 µm, range 88.33 - 113.87) and fellow (mean 98.51 ± 5.87 µm, range 87.57 - 105.77) eyes compared to control eyes (mean 105.44 ± 10.01 µm, range 96.53 - 118.27). There was no significant difference in the thickness of the inner retinal layers at the 4-degree temporal location between amblyopic and fellow eyes (p=0.73, paired t-test). IRT in amblyopic and control eyes at the 4-degree temporal location was also not significantly different (p=0.24, unpaired t-test).

(a) (b)

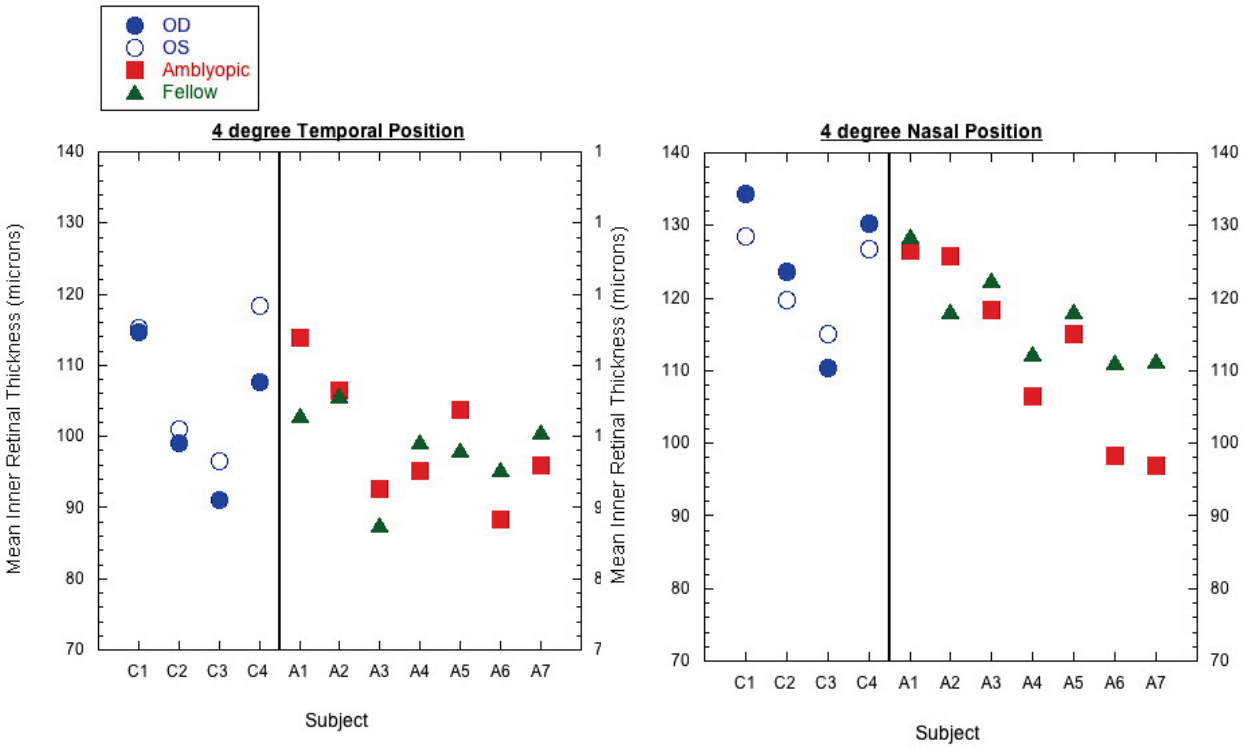


Figure 9. Individual IRT. Inter-ocular differences of IRT, shown at the 4-degree temporal position (a) and 4-degree nasal position (b) by subject. Control subjects are plotted to the left of the solid line, while amblyopic subjects are plotted to the right.

IRT values at the 4-degree nasal position were also slightly thinner in amblyopic and fellow eyes compared to control eyes, with a mean thickness in the amblyopic group of 112.49 ± 12.24 μm (range 96.90 - 126.60), 117.46 ± 6.49 μm (range 111.23 - 128.6) in fellow eyes, and 123.60 ± 8.10 μm (range 110.43 - 134.43) in the control group. However, while there was no significant difference in thickness of the inner retinal layers at the 4-degree nasal location between amblyopic and fellow eyes (paired t-test, p=0.12), the difference in IRT between amblyopic and control eyes approached significance (p=0.06, unpaired t-test). At this location, the mean IRT of control eyes was greater than amblyopic eyes. Interestingly, Figure 9b shows how both of the anisometropic subjects' (A6 and A7) thickness measurements at the 4-degree nasal position may be influencing this result. Despite a comparison of IRT with axial length parameters in this subject set shows that there was not a strong relationship between axial length and thickness measurement, there is a possibility of this influence that is not detectable due to small subject group size (See "Effect of Axial Length on OCT Measurements" section below for further discussion).

Outer Retinal Thickness (ORT)

Average ORT at the 4-degree temporal position was similar among all subject groups: 89.14 ± 5.55 μm (range 81.03 - 99.03) in control eyes, 88.57 ± 2.65 μm (range 83.47 - 90.97) in amblyopic eyes, and 88.72 ± 2.59 μm (range 85.00 - 91.93) in fellow eyes. At the 2-degree temporal position, mean ORT was also similar among subject groups: 95.87 ± 4.40 μm (range 89.77 - 103.43) in control eyes, 93.66 ± 2.70 μm (range 89.77 - 97.30) in

amblyopic eyes, and 94.60 μm ± 2.17 μm (range 92.23 - 97.57) in fellow eyes. ORT measured at the 2-degree nasal position was slightly thicker in fellow eyes compared to control and amblyopic eyes, with mean thickness measuring 96.41 ± 3.60 μm (range 92.43 - 102.53) in fellow eyes, 94.97 ± 3.34 μm (range 89.03 - 99.73) in control eyes, and 94.47 ± 2.91 μm (range 90.13 - 97.60) in amblyopic eyes. Fellow eye group thickness was also slightly greater in comparison to amblyopic and control groups at the 4-degree nasal position. At this location, mean fellow eye thickness was 91.44 ± 3.29 μm (range 87.03 - 96.73), 89.02 ± 3.39 μm (range 85.65 - 94.40) in control eyes, and 89.56 ± 4.43 μm (range 83.23 - 94.97) in amblyopic eyes. Mean ORT among subject groups at the four locations studied is shown in Table 5.

	4T	2T	2N	4N
Control	89.14±5.55	95.87±4.40	94.97±3.34	89.02±3.39
Amblyopic	88.57±2.65	93.66±2.70	94.47±2.91	89.56±4.43
Fellow	88.72±2.59	94.60±2.17	96.41±3.60	91.44±3.29

Table 5. ORT by Subject Group, in μm ± σ, at the four retinal locations studied (T=temporal, N=Nasal)

Outer retinal thickness did not significantly differ between amblyopic or control eyes at the 4-degree nasal or temporal, nor at the 2-degree nasal and temporal locations (all $p>0.10$, unpaired t-test). Figure 10 shows the difference between subject groups at the four locations studied. ORT differences between amblyopic and fellow eyes at the 4-degree temporal and nasal positions were not significant. However, there was a significant

difference in ORT between amblyopic and fellow eyes at the 2-degree nasal (p=0.03) and 2-degree temporal (p=0.02) positions.

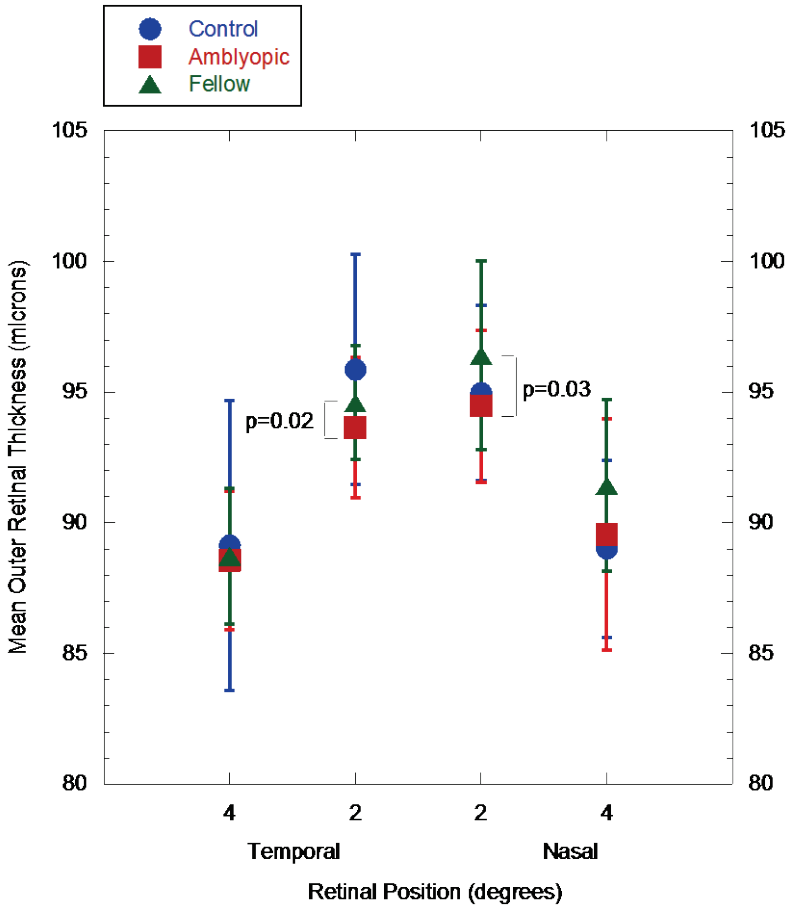


Figure 10. Mean ORT, by subject group at the four retinal locations studied

Figure 11 shows how individual inter-ocular differences appear between control and amblyopic subjects at the four locations studied. These graphs also show a general trend that the ORT of fellow eyes tends to be greater than amblyopic eyes within subjects, particularly at the 2-degree locations. However, this difference is slight, with an average difference (fellow – amblyopic eye) among subjects at the 2-degree temporal position of 0.94 ± 0.73 µm (range 0.27 - 2.47), and 1.94 ± 1.84 µm (range 0.83 - 5.97) at the 2-degree nasal position.

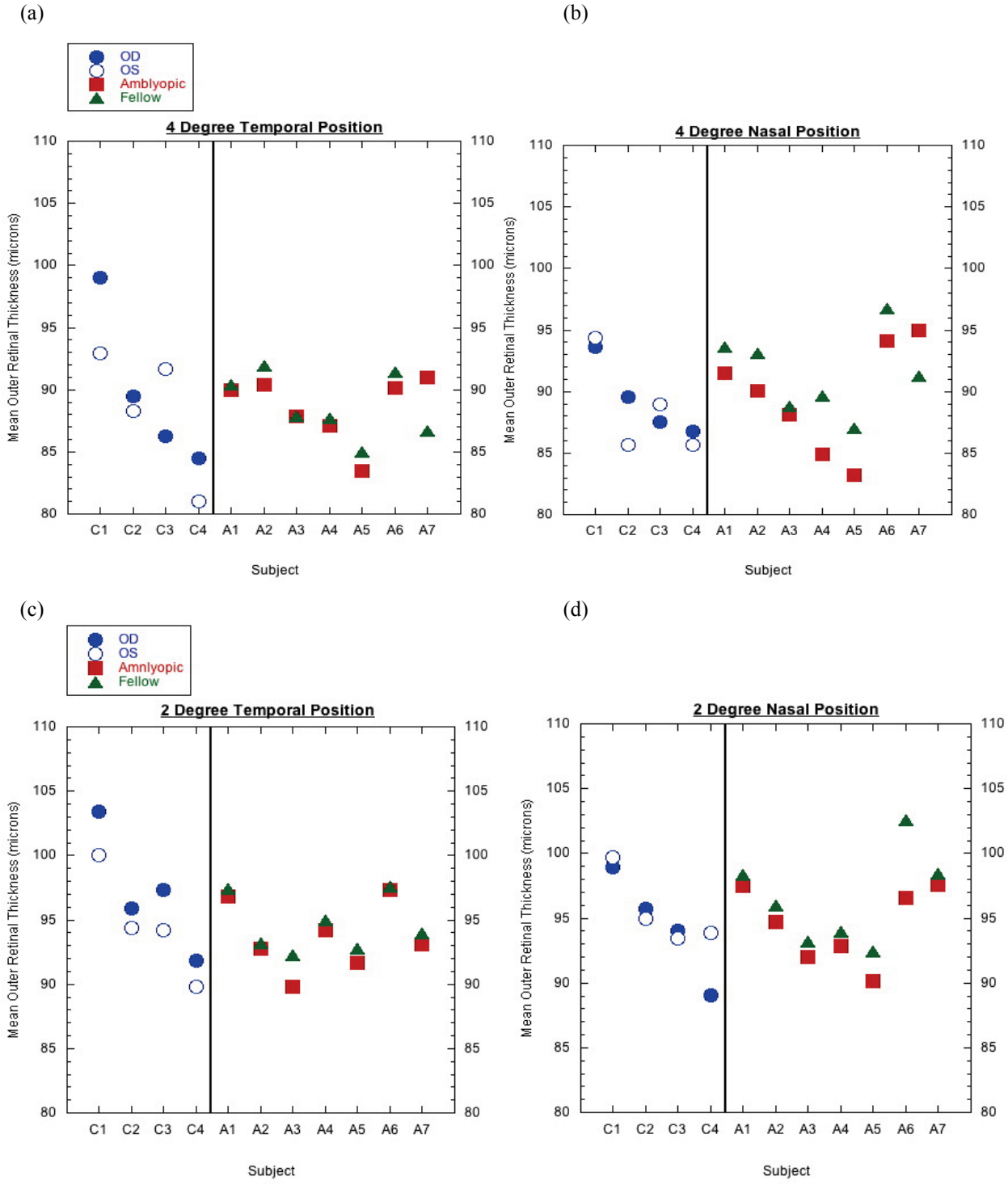
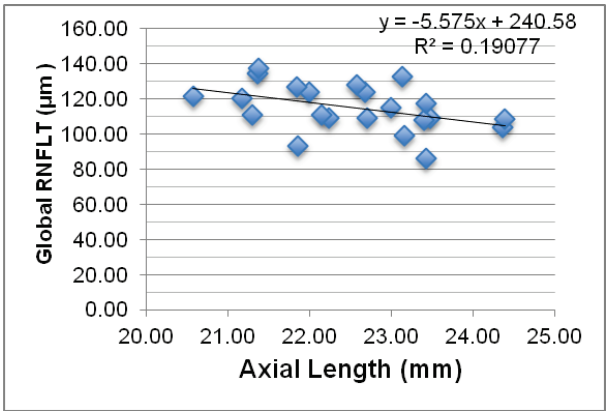


Figure 11. Individual ORT. Inter-ocular ORT plotted at the (a) 4-degree temporal (a), (b) 4-degree nasal location, (c) 2-degree temporal and (d) nasal locations by individual subject. ORT of control subjects is plotted to the left of the solid line.

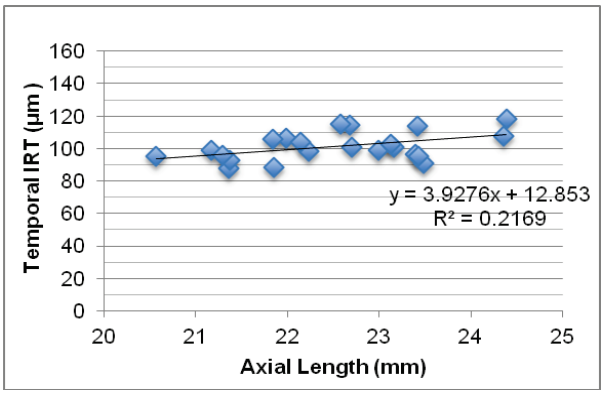
Effect of Axial Length on OCT Measurements

Thickness measurements obtained from OCT scans were examined to determine if measurements could be affected by potential magnification effects due to varying subject axial length. Although a previous study utilizing the same OCT instrumentation has shown that such effects are negligible on macular thickness,[69] consideration was taken in this study. The relationship between axial length and global RNFLT was evaluated with linear regression analysis as shown in Figure 12a. This analysis showed that only 19% of the variability (R^2=0.19) in RNFLT was explained by axial length; therefore, there was not a strong relationship between these parameters. Nor was there a strong correlation of temporal and nasal IRT measurements with axial length of subjects (R^2=0.22 and 0.23, respectively). (Figures 12b-c). There was negligible relationship of ORT measurements with axial length at the 4-degree temporal, 2-degree temporal, 2-degree nasal, and 4-degree nasal positions studied (R^2= 0.05, 0.12, 0.10, and 0.002, respectively). Thus, any differences seen in retinal thickness are not likely to be attributed to a magnification effect of OCT measurements in this study.

(a)



(b)



(c)

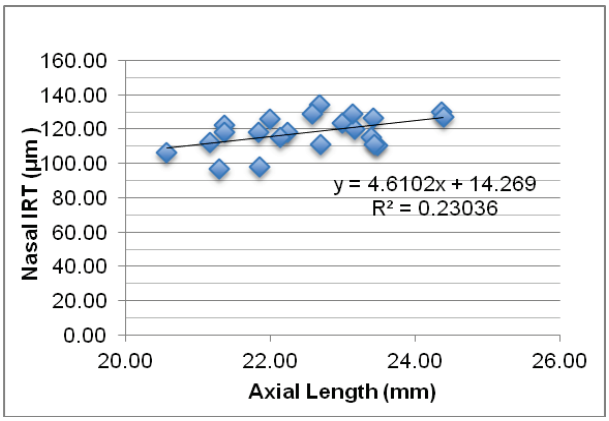


Figure 12. Retinal Thickness Measurements and Axial Length. RNFLT (a), temporal IRT (b) and nasal IRT (c) measurements tested for correlation with subjects' axial length measurements

Adaptive Optics (AO) Imaging

AO images from all 4 retinal locations were analyzed for subjects C1-C4 and A1, A5-A7. The number of images registered together ranged from 2-9, depending on the availability of similar images obtained for a given location. Images at two locations were not registered with others due to lack of repeated similar images, of subject A1 at the 4- and 2-degree nasal locations.

The cone density values from our AO images were compared against reported values from both histology data from Curcio et al.[70] and AO data from Chui et al[64] (Figure 13). As expected, mean cone density in all groups was lower at the 4-degree locations than at the 2-degree locations; i.e., cone density decreased with an increase in retinal eccentricity.

Mean cone density from amblyopic eyes fell within control subject group density ranges (mean ± standard deviation) at the 2-degree temporal, 2-degree nasal, and 4-degree nasal positions (Table 6), but was higher than the control range at the 4-degree temporal location. At this location, mean amblyopic group density was 25,247.25 cells/mm^2, which fell outside control density range (21,866.25 ± 2,097.97 cells/mm^2; see Figure 14). This difference was slight (mean amblyopic – mean control = 3,381 cells/mm^2). However, as demonstrated in Figure 13, significant variability in cone density can be observed among many subjects, regardless of subject group. Wide variability of individual cone density has been previously documented.[70] However, a preliminary analysis of how cone density might vary with the type of amblyopia showed that density of cones in the anisometropic subjects

tended to be approximately 40% more dense than mixed amblyopic (hyperopic and strabismic) subjects at all retinal locations studied except for the 4-degree temporal location.

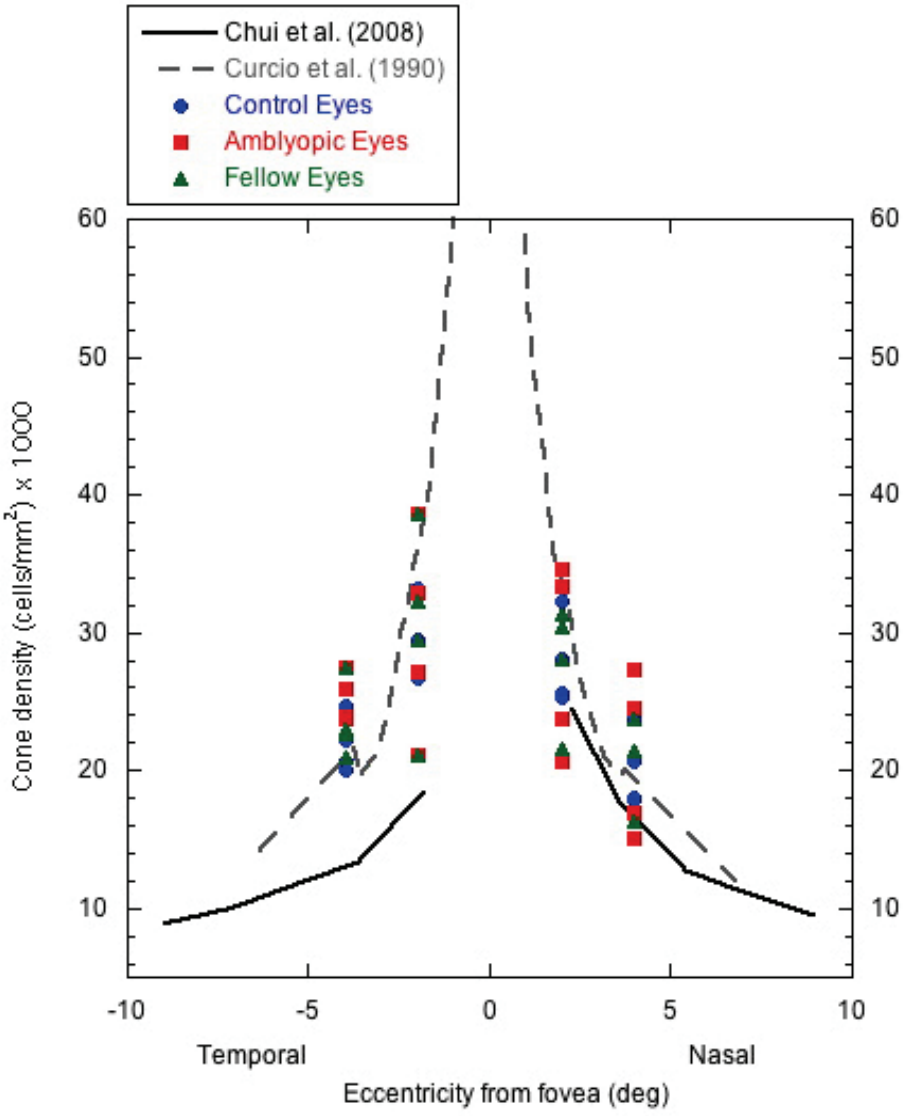


Figure 13. Cone Density Comparison. Each subject's cone density plotted against densities reported by histological[70] and AO[64] -derived studies along the horizontal retinal axis.

	4TR	2TR	2NR	4NR
C	21866.25 ± 2097.97	30642.50 ± 3098.44	27794.25 ± 3232.75	20018.75 ± 2761.51
A	25247.25 ± 1757.10	30010.00 ± 7505.72	28114.00 ± 6924.29	20973.25 ± 5923.66
F	23524.00 ± 2830.42	28252.25 ± 4856.96	28742.50 ± 5403.39	20734.25 ± 3176.63

Table 6. Subject Group Cone Density. Density values of subject groups (C=control, A= amblyopic, F= fellow), in cells/mm^3 ± σ

Another way to characterize cone photoreceptors is to investigate their packing arrangement. Figure 15 shows a Voronoi analysis of a cone mosaic taken from subject C2 at the 4-degree temporal retina, as an example. When cones are optimally packed together, they form a hexagonal array, that is, each cone is surrounded by six neighboring cones.[68]

Figure 16 shows the distribution of cones with different numbers of neighboring cones within the retinal images of control, amblyopic, and fellow eye groups at the 4-degree temporal retinal position. Figure 16 indicates that amblyopic eyes appear to be packed less regularly, shown by the wider distribution of cells that had a number of neighbors other than six (<6 or >6). However, this difference is slight and not evident by direct inspection of images. For reference, Figure 17 shows Voronoi diagrams for subject A7, in which there appears to be relative similarity between the proportions of cells with 6 neighbors.

Analysis by ANOVA testing revealed significant differences in the proportion of cells with a given number of neighbors at two retinal locations. At the 4-degree temporal location, amblyopes had a higher number of cells with only 4-neighbors ($p=0.042$) and at the 2-degree temporal location a higher number of cells with 7-neighbors ($p=0.014$).

At the 4-degree temporal position, amblyopic subjects have the highest proportion (5.99%) of cones with four neighbors over control eyes (4.70%) and fellow eyes (4.09%), (see Figure 16). This analysis suggests cones in this location are more coarsely arranged.

There was also a significant difference in the proportion of cells with 7-neighbors at the 2-degree temporal position. Control eyes have a proportion of 18.78%, amblyopic eyes 20.96% and fellow eyes with 19.55% (see Figure 18). This suggests that there is a more dense arrangement of cones in amblyopic and fellow eyes at this location.

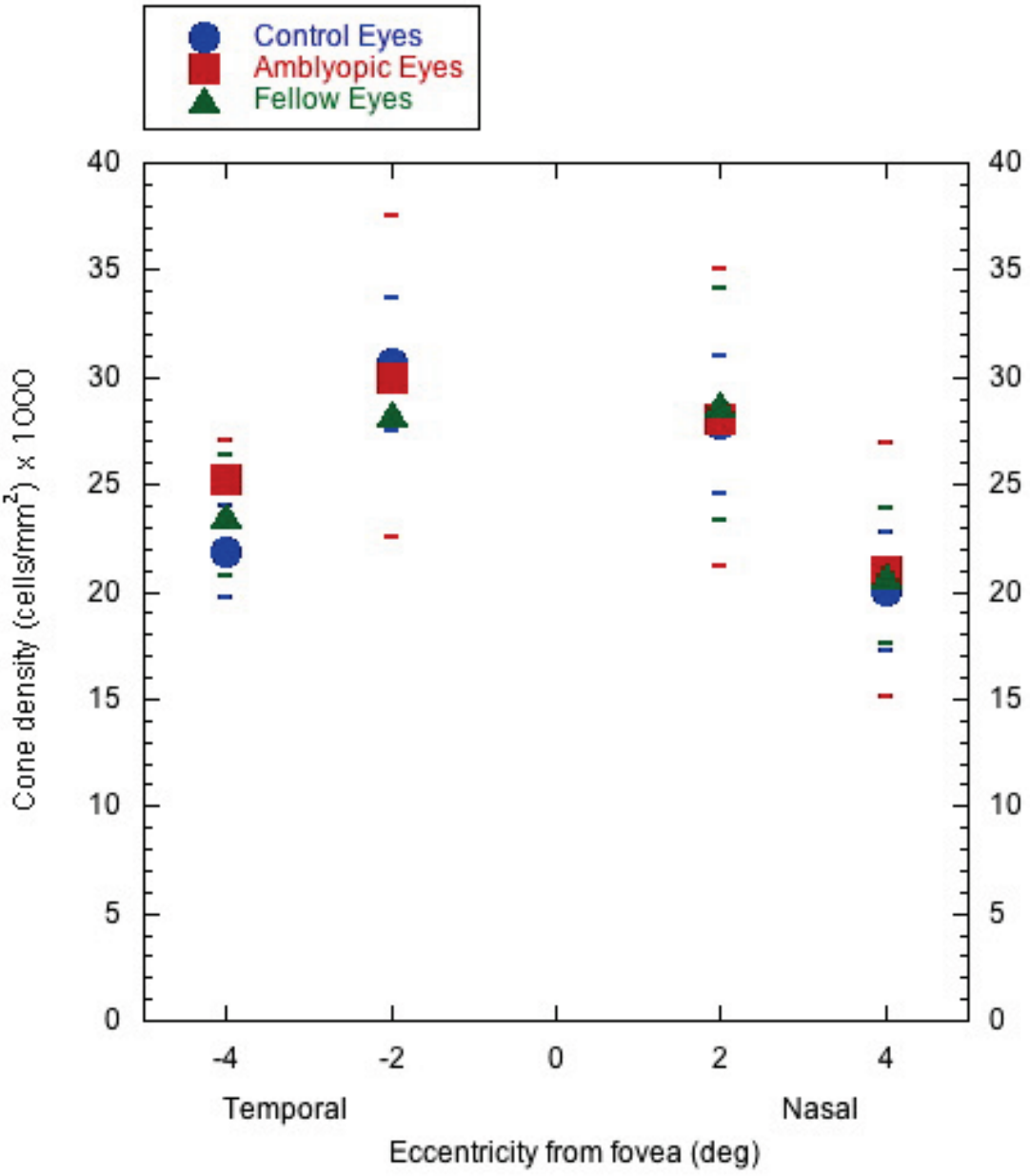
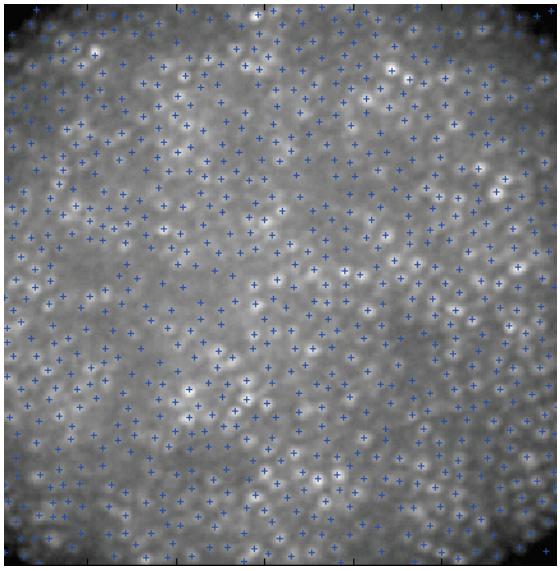
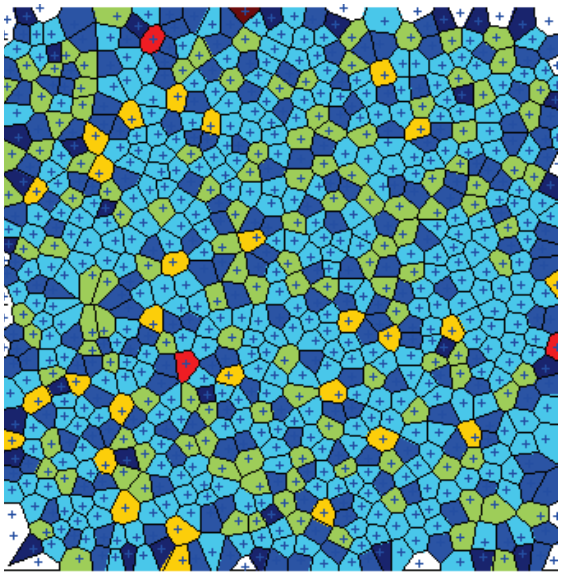


Figure 14. Mean Cone Density of Subject Groups by Retinal Position. Negative retinal position values are temporal retinal areas, while positive retinal position values are nasal retinal areas.

(a)



(b)



(c)

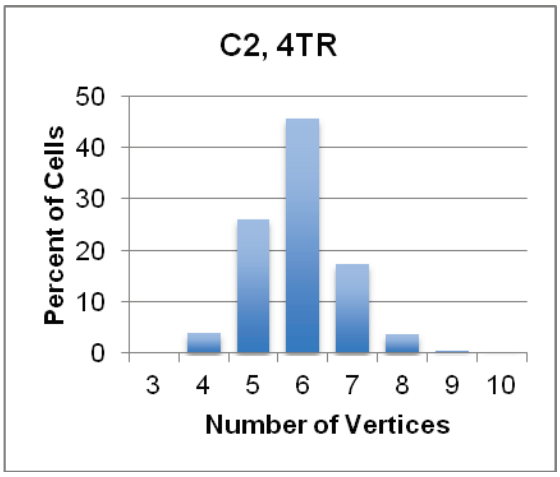
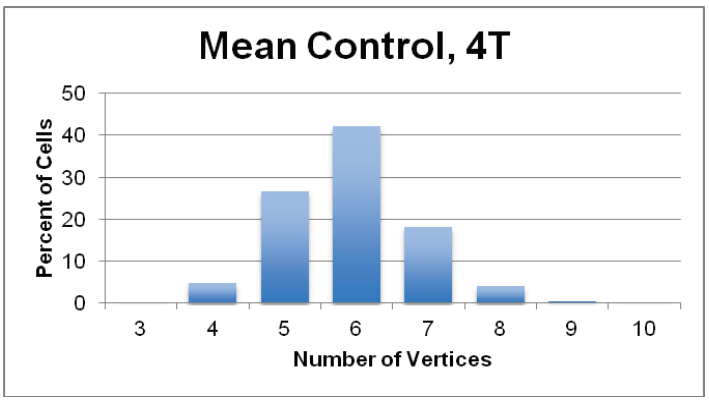
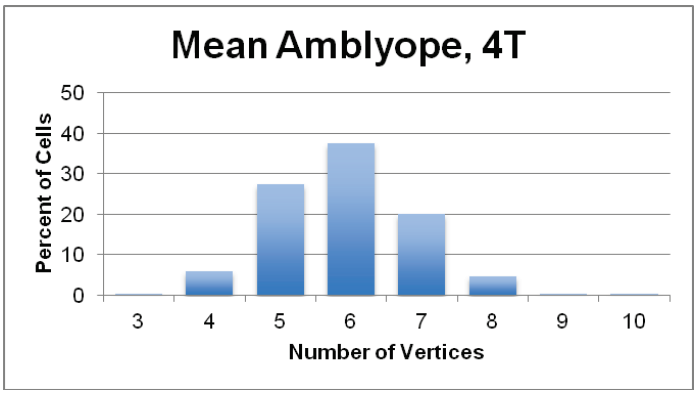


Figure 15. Cone Selection and Voronoi Analysis. AO image (a) from subject C2 (taken at 4-degree temporal retina); individual cones are accurately identified as indicated by a blue cross. Voronoi analysis (b) of figure (a) shows photoreceptors, color-coded for number of neighboring cones. The aqua color in (b) represents photoreceptors that are surrounded by 6 neighboring cones. Distribution of cones that are surrounded by various numbers of surrounding cones (vertices) is plotted in (c).

(a)



(b)



(c)

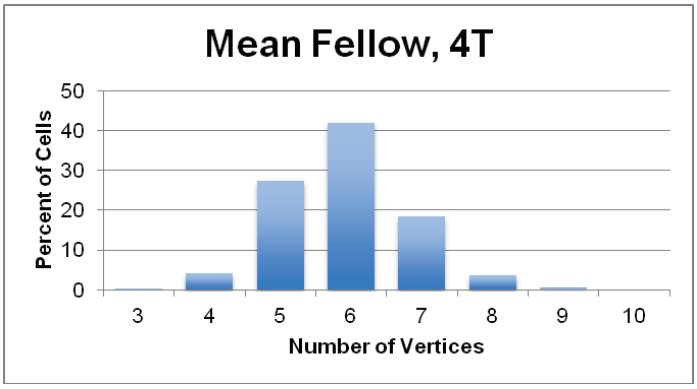
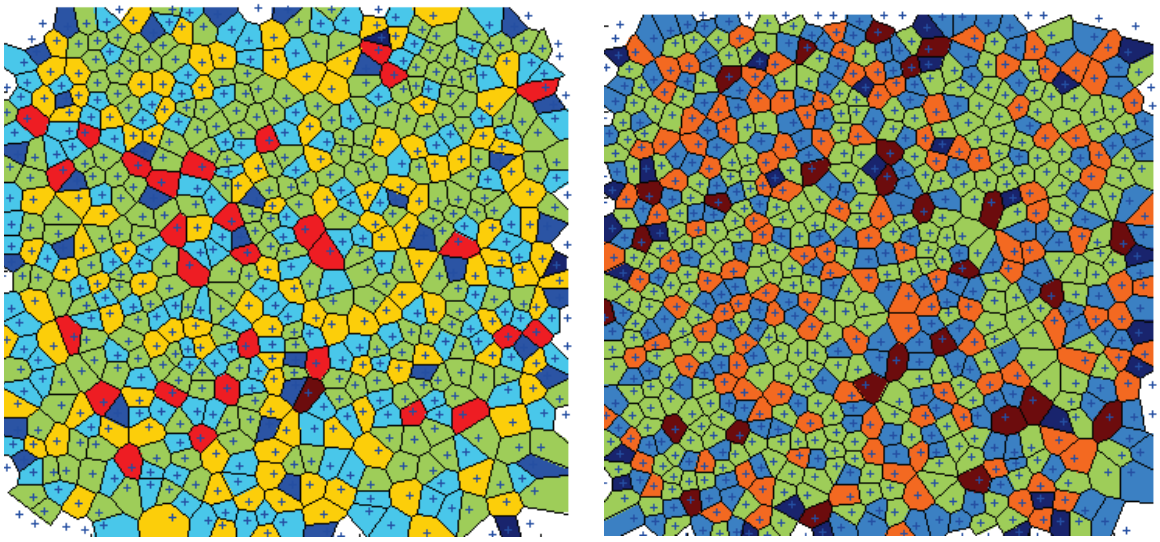


Figure 16. Voronoi Analysis at 4-degree Temporal Retina. Mean distribution of cells with a given number of neighboring cells (vertices) of (a) control subjects, (b) amblyopic subjects, and (c) fellow subjects.

(a) (b)



(c) (d)

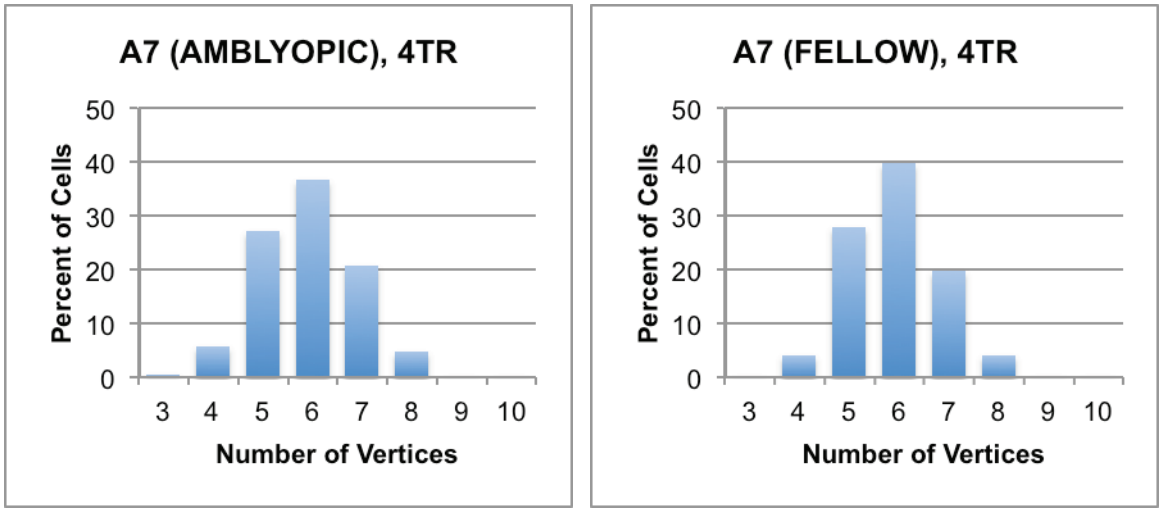
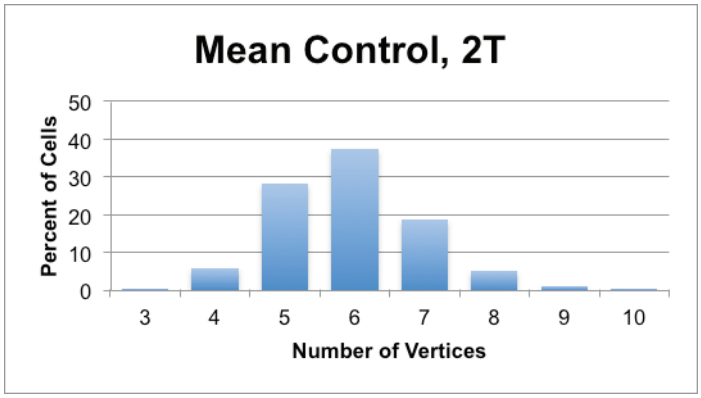
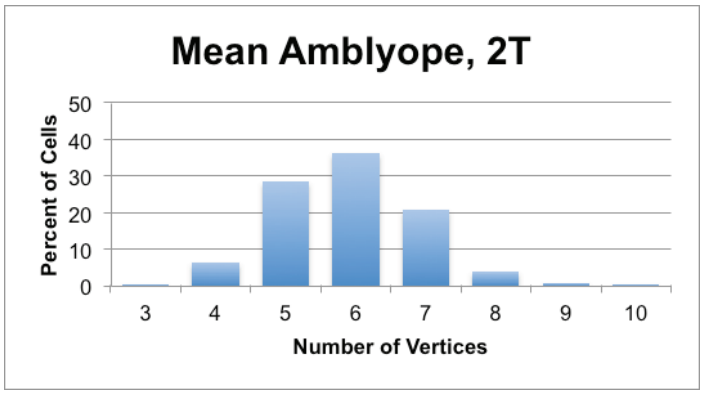


Figure 17. Voronoi Analysis in Amblyopic Subject A7. Voronoi analysis in amblyopic eye (a) and fellow eye (b) of amblyopic subject A7. The light green color in (a) and (b) represents cones with 6 surrounding neighboring cones. Distribution of cones that are surrounded by various numbers of surrounding cones is plotted for amblyopic eye (c) and fellow eye (d).

(a)



(b)



(c)

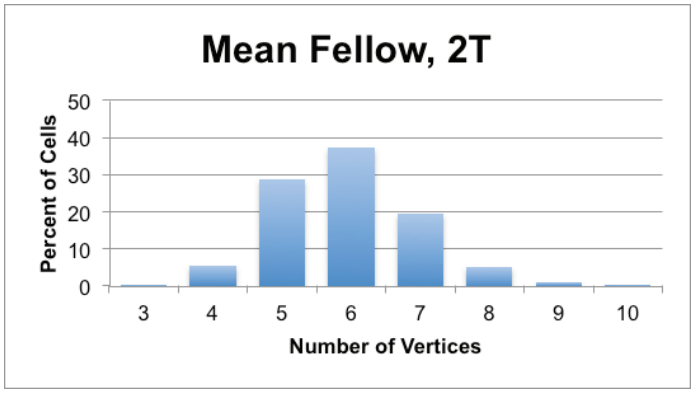


Figure 18. Voronoi Analysis at 2-degree Temporal Retina. Distribution of cones that are surrounded by various number of surrounding cones is plotted for control subjects (a), amblyopic subjects (b), and fellow subjects (c).

Discussion

Retinal Nerve Fiber Layer Thickness (RNFLT)

Yen et. al.[32] hypothesized that an increased nerve fiber layer thickness occurs in amblyopia due to a potential arrest in the natural apoptosis of retinal ganglion cells during early retinal development. Our study did not find a difference in RNFLT in our subject group to support this theory. This study did not find a significant difference in peri-papillary RNFLT in this group of amblyopic eyes compared to their fellow eyes or control subjects, which is in agreement with several other studies.[49,55–57] However, this finding is also not in agreement with other reports[32,52,54] that did find increased RNFLT in amblyopic eyes.

Different conclusions among studies investigating RNFLT in amblyopic subjects may be due to differences in subject group composition and use of different imaging instrumentation. Some studies also only investigated isolated groups of anisometropic[54] or strabismic amblyopes without anisometropia,[55] whereas some studies combined both strabismic and anisometropic amblyopes, with some studies looking at sub-group analysis secondarily. [49,51,53] The age range of subject groups in some studies may also have an effect on their results, as a correlation between age and RNFL thickness has been found, showing generalized thinning with age.[71,72] Different OCT instrumentation is also used among the studies, with older studies using a lower resolution system such as the Zeiss OCT 3 and some others using Cirrus or Spectralis instruments.

The difference in RNFLT seen in anisometropic, but not strabismic, amblyopes in some studies has led some to hypothesize that the thickness difference is attributable to difference in refractive error or axial length; as some reports cite that 1.7 μm of thickness difference is attributable to every diopter of hyperopia.[72] However, others have refuted correlation of refractive error with thickness measurements within a study of amblyopic children.[56] Some studies have exclusion criteria to avoid this type of correlation, for instance excluding patients with 1.5 D or more of anisometropia[58] or refractive errors above a certain spherical equivalent.

Analysis within our study did not show a strong correlation between axial length and RNFLT (see Figure 12a). That is, analysis by linear correlation found that axial length in this subject group only predicted about 19% of variability found in RNFLT. Moreover, the range of axial length amongst subject groups had some overlap.

Macular Thickness

While the primary outcome measure in many previous studies is macular thickness, these studies do not always measure the same positions surrounding the macula. For instance, many studies measure the average macular thickness of 10 points measured in a 6 mm diameter area around the fovea as measured with the OCT 3000 (Zeiss),[49,54,55] while some measured minimum foveal thickness as well.[49,50,54,58] This study, in contrast, investigated the thickness of specific layers in the macular area, at 2-degree and 4-degree eccentricities from the fovea, which largely are located within the 3 mm diameter macular

ring as measured in many macular scan protocols. The reason for these more precise measurements of inner and outer retinal thickness in the macular area was to more closely examine which component of the retina might be a factor in retinal changes seen, if any.

There are several issues to consider when directly comparing the macular thickness findings within this study and between studies. Firstly, the measurement of different macular areas with various models of OCT prevents direct comparison between studies. In addition, the differing profile of each study's amblyopic group also prevents the direct comparison of between group findings.

Moreover, it has been suggested[73] that there is a possibility in amblyopic eyes of measuring extra-foveal areas erroneously when using the OCT macular scan, if eccentric fixation is present. This may result in falsely higher macular thickness measurements. To consider this possibility, this study measured subjects for eccentric fixation and ensured that analysis of the OCT macular scans were centered from the patient's true fovea rather than their fixation point. The technique of using manual measurements by the OCT program's caliper tool bypasses this possible source of error, since the examiner manually selected retinal areas referenced from the foveal center.

Inner Retinal Thickness (IRT)

Thickness of the inner retinal layers was only examined at the 4-degree nasal and temporal eccentricities, as the 2-degree position was located within the para-foveal region.

At this 2-degree eccentricity from the foveal center, thickness measurements are highly influenced by foveal pit sloping characteristics and therefore can be highly variable. A recent study by Bruce et al.[41] investigated foveal pit characteristics of amblyopic eyes compared to normal control eyes. Their findings suggest that both eyes of amblyopes have a shallower foveal pit slope. While foveal pit slope was not directly measured in this study, it is unlikely that such a shallow slope could influence the nasal inner retinal layer measurements at an eccentricity as distant as 4-degrees away from the foveal center.

At the 4-degree nasal position, there was a marginally non-significant difference between amblyopic and control eyes, with amblyopic eyes slightly thinner than control subjects'. The difference is greatest amongst the two anisometropic subjects, A6 and A7. Whether this difference seen is not a factor of axial length of the anisometropic subjects per se, but a difference in the type of amblyopia, is yet to be determined.

The work by Park, et. al.[58] was one of the few other studies that investigated particular layers of the retina in amblyopes and reported thinning of inner retinal layers (ganglion cell layer plus inner plexiform layer) in amblyopic eyes at certain macular locations studied. This thinning of the inner retinal layers within the area of inner retina studied here (RNFL plus layers studied by Park[58]) is consistent with and in the same direction as found in this study.

Outer Retinal Thickness (ORT)

Thickness of the outer retinal layers at both the 2-degree nasal and 2-degree temporal positions was found to be significantly different between amblyopic and fellow eyes, but not compared to control eyes. While this difference was statistically significant, the mean difference of ORT was about 1-2 μm, which is not likely to be of any clinical significance and likely within measurement error. This finding appears to correlate with the cone density measurements observed, as mean amblyopic cone density in all subject groups is nearly identical at the two nasal positions studied, and there is no consistent pattern of density difference at the temporal locations.

Adaptive Optics (AO) Imaging

The photoreceptors are the first cell to respond to light in the visual system; therefore any effect resulting from an amblyogenic visual experience would be a retrograde effect from later processing in the visual system. There did not, however, appear to be any meaningful differences in cone density measurements between subject groups in this study.

Photoreceptor density measurements in this study agreed fairly well with both published histological and AO-derived density measurements (see Figure 13). Density values in the temporal retina in this study were higher than the values found in controls of another study[64] using AO across all subject groups. While previous studies have shown differences in cone density measurements as a result of differences in axial length,[64,74] the

difference between mean axial length in the amblyopic and fellow eyes of this study (21.80 and 22.27 mm, respectively) versus that in emmetropic eyes (23.38 mm) is likely not great enough to demonstrate significant differences in this area, as one study reported a decrease of 341 cones/mm^2 per 1 mm increase in axial length.[74]

Deviations from a hexagonal arrangement suggests a coarser arrangement of cones in the retina; analysis of the number of neighbors surrounding each cone can lead to inferences about the organization of the retina in a given retinal location. While analysis of packing characteristics of photoreceptors in amblyopic eyes suggested that there appears to be less organization of the cone mosaic in amblyopic eyes, these findings were isolated to two locations and significant only for difference in proportion of cells with four neighboring cells (4-degree temporal), and seven neighboring cells (2-degree temporal). Thus, there was some suggestion of denser packing in amblyopic eyes at the 2-degree temporal location with a higher proportion of cells with 7 neighboring cones, and coarser packing at the 4-degree temporal location, with a higher percentage of cones having 4 neighboring cones. These findings are of interest as they suggest that the cone mosaic of amblyopic eyes may deviate slightly from the expected hexagonal array. While these differences are found to be statistically significant, the clinical and anatomical significance of these small differences remains to be seen.

Correlation to Visual Function

When studying retinal characteristics in amblyopia, the question of any association of retinal morphology with visual function is a worthy question. The main outcomes of the visual function testing used in this study were optotype visual acuity, the presence of monofixation or central suppression, and stereopsis. Two of the subjects in this study (A1 and A6) had poor visual acuity, despite a history of early treatment (A1), and in the absence of treatment in childhood. (A6). The retinal findings of these two subjects in terms of RNFLT, macular thickness or cone density in these subjects did not share meaningful differences from the other amblyopic subjects in this study.

While measurement errors due to non-foveal fixation behavior were eliminated in studying retinal thickness measurements obtained by OCT imaging due to the nature of the techniques used to evaluate thickness measurements, imaging by AO relied on subjects' fixation to an external target. Therefore, if subjects used a non-foveal point to fixate, the retinal location imaged was potentially deviated from the location of interest by the amount of eccentric fixation, assuming fixation was relatively stable. However, it did not appear that the cone density measurements in amblyopic subjects were shifted by values that would indicate nasal eccentric fixation.

Limitations

Due to the small population sample that this study recruited from and the more rare nature of amblyopia in the general population, the number of subjects that participated in the study was a major limitation. Furthermore, the etiology of amblyopia in most subjects of this study was mixed, that is, many subjects had both strabismus and hyperopic anisometropia, so any differences in retinal characteristics between amblyopia type were not segregated in analysis. Furthermore, not all subjects that were recruited to the study were able to participate in AO imaging. This was mainly due to their declining to undergo cycloplegia due to the side effects in our highly hyperopic subjects or due to individual time constraints.

In addition, the majority of adult amblyopic subjects in this study had a history of treatment, with generally successful visual acuity outcomes. Therefore, it is difficult to ascertain what effect treatment may have had on retinal development or changes resulting from amblyogenic risk factors in the absence of treatment. As the process of amblyopia develops and is typically treated in early childhood, it would be more elucidating to collect data on retinal characteristics in this age group. Unlike AO fundus cameras, AO-scanning laser ophthalmoscope (AO-SLO) imaging takes images of cones at a video rate; hence, AO-SLO would be a more suitable modality for a younger population.

Having multiple examiners perform caliper measurements of OCT images and cone density analysis in a masked fashion and examining intra-observer variability between the manual and software approaches would have added strength to the results of this study. Due to the small size and nature of this preliminary study, this was not possible. However, the

use of the custom software program used to calculate cone density has been validated by a previous study.[75]

Future Work

As a recent study suggests differences in foveal slope dimensions in amblyopic eyes,[41] investigating foveal pit geometry may prove interesting. It is possible that difference in this retinal component may have an influence on total average macular thickness and positional thickness of retinal layers.

The visual experience in strabismic versus anisometropic amblyopia is different and different visual function and retinal characteristics have been reported in each of these types of amblyopia. Preliminary analysis in this study's small subject group suggested increased cone density in the anisometropic amblyopic eyes as compared to mixed amblyopic eyes, a finding that can only be anecdotal at this point due to small sample size. Thus, analyzing retinal characteristics such as retinal thickness and cone characteristics as compared to control and fellow eyes should be ideally carried out within these two amblyopic subject groups. Analysis regarding this type of amblyopia on a larger scale would carry more power and sensitivity in detecting any retinal differences in different mechanisms of amblyopia. Furthermore, carrying out analyses of visual function as correlated to retinal characteristics in amblyopic eyes based on amblyopia type may be beneficial to identify a relationship to functional deficits, if any exist.

Tracking retinal characteristics during the time course of amblyopia diagnosis and subsequent treatment has value in elucidating any presenting differences in amblyopia and observing any changes due to treatment. One such study has used OCT thus far to evaluate overall macular thickness in isoametropic hyperopic amblyopia, finding thinning of the fovea during treatment but without association with improvement in visual acuity.[76] The use of AO-SLO to further investigate cone characteristics in a larger subject group, as well as in children at various states of treatment can be better used to evaluate cone characteristics in this population in conjunction with OCT-derived thickness data. Additionally, AO-SLO may have the potential to be used as an alternative technique to examine fixation behavior in amblyopes demonstrating monofixation syndrome.

Conclusions

While this study found slight differences in outer retinal thickness between amblyopic and fellow eyes, and some suggestion of difference in the nasal inner retinal layers, we did not find any indication that RNFLT is altered in amblyopia. Preliminary AO data suggest that while no differences in cone density may exist, the cone packing characteristics may be more disorganized in amblyopic eyes. The identification of any retinal differences in amblyopic eyes has implications in the understanding of how visual disturbance may affect retinal development. Furthermore, identifying retinal differences and whether these characteristics are permanent or changeable may prove useful in determining prognosis and tracking progress of amblyopia treatment.

Bibliography

1. Ciuffreda K, Levi D, Selenow A. *Amblyopia : basic and clinical aspects*. Boston: Butterworth-Heinemann; 1991.

2. Sernagor E, Eglen S, Harris B, Wong R. *Retinal development*. Cambridge: Cambridge University Press; 2006.

3. Robaei D, Rose KA, Ojaimi E, Kifley A, Martin FJ, Mitchell P. Causes and associations of amblyopia in a population-based sample of 6-year-old Australian children. *Arch. Ophthalmol.* 2006;124(6):878–884. doi:10.1001/archopht.124.6.878.

4. Kvarnström G, Jakobsson P, Lennerstrand G. Visual screening of Swedish children: an ophthalmological evaluation. *Acta Ophthalmol Scand*. 2001;79(3):240–244.

5. Newman DK, East MM. Prevalence of amblyopia among defaulters of preschool vision screening. *Ophthalmic Epidemiol*. 2000;7(1):67–71.

6. Multi-Ethnic Pediatric Eye Disease Group (MEPEDS). Prevalence of Amblyopia and Strabismus in African American and Hispanic Children Ages 6 to 72 Months. *Ophthalmology*. 2008;115(7):1229–1236.e1. doi:10.1016/j.ophtha.2007.08.001.

7. Friedman DS, Repka MX, Katz J, et al. Prevalence of amblyopia and strabismus in white and African American children aged 6 through 71 months the Baltimore Pediatric Eye Disease Study. *Ophthalmology*. 2009;116(11):2128–2134.e1–2. doi:10.1016/j.ophtha.2009.04.034.

8. Dana MR, Tielsch JM, Enger C, Joyce E, Santoli JM, Taylor HR. Visual impairment in a rural Appalachian community. Prevalence and causes. *JAMA*. 1990;264(18):2400–2405.

9. Wang JJ, Foran S, Mitchell P. Age-specific prevalence and causes of bilateral and unilateral visual impairment in older Australians: the Blue Mountains Eye Study. *Clin. Experiment. Ophthalmol.* 2000;28(4):268–273.

10. Chua B. Consequences of amblyopia on education, occupation, and long term vision loss. *British Journal of Ophthalmology*. 2004;88(9):1119–1121. doi:10.1136/bjo.2004.041863.

11. Donahue SP, Arthur B, Neely DE, Arnold RW, Silbert D, Ruben JB. Guidelines for automated preschool vision screening: A 10-year, evidence-based update. *J AAPOS*. 2013. doi:10.1016/j.jaapos.2012.09.012.

12. Massachusetts Department of Public Health. Massachusetts Vision Screening Protocols Memorandum. 2005. Available at: http://www.mass.gov/eohhs/docs/dph/com-health/school/vision-letter.pdf.

13. Holmes JM, Repka MX, Kraker RT, Clarke MP. The Treatment of Amblyopia. *Strabismus*. 2006;14(1):37–42. doi:10.1080/09273970500536227.

14. Holmes JM, Lazar EL, Melia BM, et al. Effect of age on response to amblyopia treatment in children. *Arch. Ophthalmol.* 2011;129(11):1451–1457. doi:10.1001/archophthalmol.2011.179.

15. Scheiman MM, Hertle RW, Beck RW, et al. Randomized trial of treatment of amblyopia in children aged 7 to 17 years. *Arch. Ophthalmol*. 2005;123(4):437–447. doi:10.1001/archopht.123.4.437.

16. Wiesel TN, Hubel DH. Single-cell Responses in Striate Cortex of Kittens Deprived of Vision in One Eye. *J. Neurophysiol*. 1963;26:1003–1017.

17. Wiesel TN, Hubel DH. Comparison of the effects of unilateral and bilateral eye closure on cortical unit responses in kittens. *J. Neurophysiol*. 1965;28(6):1029–1040.

18. Daw NW, Fox K, Sato H, Czepita D. Critical period for monocular deprivation in the cat visual cortex. *J. Neurophysiol*. 1992;67(1):197–202.

19. Horton JC, Stryker MP. Amblyopia induced by anisometropia without shrinkage of ocular dominance columns in human striate cortex. *Proc. Natl. Acad. Sci. U.S.A*. 1993;90(12):5494–5498.

20. Imamura K, Fischer H, Lennerstrand G, et al. Reduced activity in the extrastriate visual cortex of individuals with strabismic amblyopia. *Neuroscience Letters*. 1997;225(3):173–176. doi:10.1016/S0304-3940(97)00211-5.

21. Von Noorden GK, Crawford ML. The lateral geniculate nucleus in human strabismic amblyopia. *Invest. Ophthalmol. Vis. Sci*. 1992;33(9):2729–2732.

22. Purves D, Augustine G, Fitzpatrick D. *Neuroscience*. 2nd ed. Sunderland, MA: Sinauer Associates; 2001. Available at: http://www.ncbi.nlm.nih.gov/books/NBK10885/.

23. Hubel, David H. *Eye, Brain, and Vision*. New York: Scientific American Library; 1995.

24. Ikeda H, Tremain KE. Amblyopia occurs in retinal ganglion cells in cats reared with convergent squint without alternating fixation. *Exp Brain Res*. 1979;35(3):559–582.

25. Hess RF. Amblyopia: site unseen. *Clinical and Experimental Optometry*. 2001;84(6):321–336. doi:10.1111/j.1444-0938.2001.tb06604.x.

26. Williams C, Papakostopoulos D. Electro-oculographic abnormalities in amblyopia. *British Journal of Ophthalmology*. 1995;79(3):218–224. doi:10.1136/bjo.79.3.218.

27. Parisi V, Scarale ME, Balducci N, Fresina M, Campos EC. Electrophysiological Detection of Delayed Postretinal Neural Conduction in Human Amblyopia. *Investigative Ophthalmology & Visual Science*. 2010;51(10):5041–5048. doi:10.1167/iovs.10-5412.

28. Delint PJ, Weissenbruch C, Berendschot TT, Norren DV. Photoreceptor function in unilateral amblyopia. *Vision Res*. 1998;38(4):613–617.

29. Enoch JM. Amblyopia and the Stiles-Crawford effect. *American Journal of Optometry & Archives of American Academy of Optometry*. 1957;34(6):298–309.

30. Enoch JM. Further studies on the relationship between amblyopia and the Stiles-Crawford effect. *American Journal of Optometry & Archives of American Academy of Optometry*. 1959;36(3):111–128.

31. Hendrickson AE, Yuodelis C. The morphological development of the human fovea. *Ophthalmology*. 1984;91(6):603–612.

32. Yen M-Y. Retinal Nerve Fiber Layer Thickness in Unilateral Amblyopia. *Investigative Ophthalmology & Visual Science*. 2004;45(7):2224–2230. doi:10.1167/iovs.03-0297.

33. Scheetz AJ, Williams RW, Dubin MW. Severity of ganglion cell death during early postnatal development is modulated by both neuronal activity and binocular competition. *Vis. Neurosci*. 1995;12(4):605–610.

34. Jeyarasasingam G, Snider CJ, Ratto GM, Chalupa LM. Activity-regulated cell death contributes to the formation of ON and OFF alpha ganglion cell mosaics. *J. Comp. Neurol*. 1998;394(3):335–343.

35. Von Noorden GK, Crawford ML, Middleditch PR. Effect of lid suture on retinal ganglion cells in Macaca mulatta. *Brain Res.* 1977;122(3):437–444.

36. Fifková E. Effect of visual deprivation and light on synapses of the inner plexiform layer. *Exp. Neurol.* 1972;35(3):458–469.

37. Rasch E, Swift H, Riesen AH, Chow KL. Altered structure and composition of retinal cells in darkreared mammals. *Exp. Cell Res.* 1961;25:348–363.

38. Lempert P, Porter L. Dysversion of the optic disc and axial length measurements in a presumed amblyopic population. *J AAPOS.* 1998;2(4):207–213.

39. Lempert P. Optic Disc Area and Retinal Area in Amblyopia. *Seminars in Ophthalmology*. 2008;23(5-6):302–306. doi:10.1080/08820530802505997.

40. Miki A. Optic disc measurements using the Heidelberg Retina Tomograph in amblyopia. *Clinical Ophthalmology*. 2010:1025. doi:10.2147/OPTH.S13143.

41. Bruce A, Pacey IE, Bradbury JA, Scally AJ, Barrett BT. Bilateral Changes in Foveal Structure in Individuals with Amblyopia. *Ophthalmology*. 2013;120(2):395–403. doi:10.1016/j.ophtha.2012.07.088.

42. Pineles SL, Demer JL. Bilateral Abnormalities of Optic Nerve Size and Eye Shape in Unilateral Amblyopia. *American Journal of Ophthalmology*. 2009;148(4):551–557.e2. doi:10.1016/j.ajo.2009.05.007.

43. Barrett BT, Bradley A, McGraw PV. Understanding the Neural Basis of Amblyopia. *neuroscientist*. 2004;10(2):106–117. doi:10.1177/1073858403262153.

44. Agervi P, Nilsson M, Martin L. Foveal function in children treated for amblyopia. *Acta Ophthalmologica*. 2010;88(2):222–226. doi:10.1111/j.1755-3768.2008.01432.x.

45. Vincent SJ, Collins MJ, Read SA, Carney LG. Monocular amblyopia and higher order aberrations. *Vision Research*. 2012;66:39–48. doi:10.1016/j.visres.2012.06.016.

46. Ciuffreda KJ, Hokoda SC, Hung GK, Semmlow JL, Selenow A. Static aspects of accommodation in human amblyopia. *Am J Optom Physiol Opt*. 1983;60(6):436–449.

47. McKee SP, Levi DM, Movshon JA. The pattern of visual deficits in amblyopia. *J Vis*. 2003;3(5):380–405. doi:10:1167/3.5.5.

48. Levi DM, McKee SP, Movshon JA. Visual deficits in anisometropia. *Vision Res.* 2011;51(1):48–57. doi:10.1016/j.visres.2010.09.029.

49. Kee, Lee S-Y, Lee Y-C. Thicknesses of the fovea and retinal nerve fiber layer in amblyopic and normal eyes in children. *Korean J Ophthalmol*. 2006;20(3):177–181.

50. Huynh SC, Samarawickrama C, Wang XY, et al. Macular and Nerve Fiber Layer Thickness in Amblyopia: The Sydney Childhood Eye Study. *Ophthalmology*. 2009;116(9):1604–1609. doi:10.1016/j.ophtha.2009.03.013.

51. Dickmann A, Petroni S, Salerni A, Dell'Omo R, Balestrazzi E. Unilateral amblyopia: An optical coherence tomography study. *Journal of American Association for Pediatric Ophthalmology and Strabismus*. 2009;13(2):148–150. doi:10.1016/j.jaapos.2008.10.009.

52. Aguirre F, Mengual E, Hueso JR, Moya M. Comparison of normal and amblyopic retinas by optical coherence tomography in children. *Eur J Ophthalmol*. 2010;20(2):410–418.

53. Al-Haddad CE, EL Mollayess GM, Cherfan CG, Jaafar DF, Bashshur ZF. Retinal nerve fibre layer and macular thickness in amblyopia as measured by spectral-domain optical

coherence tomography. *British Journal of Ophthalmology*. 2011. doi:10.1136/bjo.2010.195081.

54. Yoon SW, Park WH, Baek S-H, Kong SM. Thicknesses of macular retinal layer and peripapillary retinal nerve fiber layer in patients with hyperopic anisometropic amblyopia. *Korean J Ophthalmol*. 2005;19(1):62–67.

55. Altintas O, Yüksel N, Ozkan B, Caglar Y. Thickness of the retinal nerve fiber layer, macular thickness, and macular volume in patients with strabismic amblyopia. *J Pediatr Ophthalmol Strabismus*. 2005;42(4):216–221.

56. Repka MX, Kraker RT, Tamkins SM, Suh DW, Sala NA, Beck RW. Retinal Nerve Fiber Layer Thickness in Amblyopic Eyes. *American Journal of Ophthalmology*. 2009;148(1):143–147. doi:10.1016/j.ajo.2009.01.015.

57. Miki A, Shirakashi M, Yaoeda K, et al. Retinal nerve fiber layer thickness in recovered and persistent amblyopia. *OPTH*. 2010:1061. doi:10.2147/OPTH.S13145.

58. Park K-A, Park DY, Oh SY. Analysis of spectral-domain optical coherence tomography measurements in amblyopia: a pilot study. *British Journal of Ophthalmology*. 2011. doi:10.1136/bjo.2010.192765.

59. Doble N. High-resolution, in vivo retinal imaging using adaptive optics and its future role in ophthalmology. *Expert Rev Med Devices*. 2005;2(2):205–216. doi:10.1586/17434440.2.2.205.

60. Wolfing JI, Chung M, Carroll J, Roorda A, Williams DR. High-Resolution Retinal Imaging of Cone–Rod Dystrophy. *Ophthalmology*. 2006;113(6):1014–1019.e1. doi:10.1016/j.ophtha.2006.01.056.

61. Choi SS, Doble N, Hardy JL, et al. In Vivo Imaging of the Photoreceptor Mosaic in Retinal Dystrophies and Correlations with Visual Function. *Investigative Ophthalmology & Visual Science*. 2006;47(5):2080–2092. doi:10.1167/iovs.05-0997.

62. Choi SS, Zawadzki RJ, Lim MC, et al. Evidence of outer retinal changes in glaucoma patients as revealed by ultrahigh-resolution in vivo retinal imaging. *British Journal of Ophthalmology*. 2010;95(1):131–141. doi:10.1136/bjo.2010.183756.

63. Choi SS, Zawadzki RJ, Keltner JL, Werner JS. Changes in Cellular Structures Revealed by Ultra-high Resolution Retinal Imaging in Optic Neuropathies. *Investigative Ophthalmology & Visual Science*. 2008;49(5):2103–2119. doi:10.1167/iovs.07-0980.

64. Chui TYP, Song H, Burns SA. Individual variations in human cone photoreceptor packing density: variations with refractive error. *Invest. Ophthalmol. Vis. Sci*. 2008;49(10):4679–4687. doi:10.1167/iovs.08-2135.

65. Flom MC, Weymouth FW, Kahneman D. Visual Resolution and Contour Interaction. *J Opt Soc Am*. 1963;53:1026–1032.

66. Bonneh Y, Sagi D, Polat U. Local and non-local deficits in amblyopia: acuity and spatial interactions. *Vision Research*. 2004;44(27):3099–3110. doi:10.1016/j.visres.2004.07.031.

67. Chauhan DS, Marshall J. The interpretation of optical coherence tomography images of the retina. *Invest. Ophthalmol. Vis. Sci.* 1999;40(10):2332–2342.

68. Li KY, Roorda A. Automated identification of cone photoreceptors in adaptive optics retinal images. *J Opt Soc Am A Opt Image Sci Vis*. 2007;24(5):1358–1363.

69. Harb E, Hyman L, Fazzari M, Gwiazda J, Marsh-Tootle W. Factors associated with macular thickness in the COMET myopic cohort. *Optom Vis Sci*. 2012;89(5):620–631. doi:10.1097/OPX.0b013e318251293a.

70. Curcio CA, Sloan KR, Kalina RE, Hendrickson AE. Human photoreceptor topography. *J. Comp. Neurol*. 1990;292(4):497–523. doi:10.1002/cne.902920402.

71. Girkin CA, McGwin G, Sinai MJ, et al. Variation in Optic Nerve and Macular Structure with Age and Race with Spectral-Domain Optical Coherence Tomography. *Ophthalmology*. 2011;118(12):2403–2408. doi:10.1016/j.ophtha.2011.06.013.

72. Salchow DJ, Oleynikov YS, Chiang MF, et al. Retinal Nerve Fiber Layer Thickness in Normal Children Measured with Optical Coherence Tomography. *Ophthalmology*. 2006;113(5):786–791. doi:10.1016/j.ophtha.2006.01.036.

73. Leone J, Koklanis K, Georgievski Z, Wilkinson R. Macular and retinal nerve fibre layer thickness in strabismus and anisometropic amblyopia. *Binocul Vis Strabismus Q*. 2008;23(4):227–234.

74. Park SP, Chung JK, Greenstein V, Tsang SH, Chang S. A study of factors affecting the human cone photoreceptor density measured by adaptive optics scanning laser ophthalmoscope. *Exp. Eye Res.* 2013;108:1–9. doi:10.1016/j.exer.2012.12.011.

75. Xue B, Choi SS, Doble N, Werner JS. Photoreceptor counting and montaging of en-face retinal images from an adaptive optics fundus camera. *J Opt Soc Am A Opt Image Sci Vis*. 2007;24(5):1364–1372.

76. Chen W, Chen J, Zhang F, Zhu X, Lu F. Visual outcome in isoametropic amblyopic children with high hyperopia and the effect of therapy on retinal thickness. *Am. J. Ophthalmol.* 2013;155(3):536–543.e1. doi:10.1016/j.ajo.2012.09.028.

Addendum 1.

Questionnaire for Potential Amblyopic Subjects (NECO and external)

Ultrahigh resolution retinal imaging of normal and amblyopic eyes using adaptive optics

Name: **DOB:** **Gender:** **M** **F**

Amblyopia History:

1. When were you first diagnosed with amblyopia?_____
2. Do you know the cause of the amblyopia?_____
3. Did you wear glasses or contact lenses when you were a child? Yes No
   a. If so, how old were you when you started wearing them? _____
   b. Did you wear your glasses all day except at bed and during bathing?_____
4. Do you wear glasses or contact lenses now? Yes No
   a. If yes, for what reason?_____
   b. If no, at what age did you stop wearing glasses?_____
5. Did you ever patch an eye? Yes No
   a. If so, on which eye?_____
   b. If so, for what ages?_____
   c. If so, approximately how many hours a day?_____
6. Did you ever have an eyeturn (strabismus)? Yes No
   a. If so, do you feel you still have one now? Yes No
   b. If so, did you ever have eye surgery and if so at what age?_____

      _____
   c. If you still feel your eye turns, please describe if and when you notice your eye turning;

      _____

      _____
7. Do you feel that you see better out of one eye and if so which?_____
8. As a child how often would you see an eye doctor?_____